LITHOS 446-447 (2023) 107135

Contents lists available at ScienceDirect

LITHOS

journal homepage: www.elsevier.com/locate/lithos

Trace element composition of micas from rare-metal granites of different geochemical affiliations

Karel Breiter[a,b,*], Michaela Vašinová Galiová[a,c], Michaela Hložková[a,d], Zuzana Korbelová[b], Jindřich Kynický[a], Hilton Tulio Costi[e]

[a] *BIC Brno, Purkyňova 125, CZ-61200 Brno, Czech Republic*
[b] *Institute of Geology, Czech Academy of Sciences, Rozvojová 269, CZ-16500, Praha 6, Czech Republic*
[c] *Institute of Chemistry and Technology of Environmental Protection, Faculty of Chemistry, Brno University of Technology, Purkyňova 118, CZ-61200 Brno, Czech Republic*
[d] *Department of Chemistry, Faculty of Science, Masaryk University, Kotlářská 2, CZ-611 37 Brno, Czech Republic*
[e] *Museu Paraense Emílio Goeldi, CP, 66075-100 Belém, PA, Brazil*

ARTICLE INFO

Keywords:
Mica chemistry
Rare-metal granite
Laser-ablation ICP-MS mineral analysis

ABSTRACT

About 2600 spot analyses of mica (combined electron microprobe and laser ablation ICP-MS) from 120 samples from eight rare-metal granite (RMG) plutons of different geochemical affiliations were performed to characterize the contents of major (Si, Ti, Al, Fe, Mn, Mg, Ca, Na, K, F), minor (Li, Rb, Zn), and trace elements (Sc, Nb, Sn, Cs, Ta, W). This allowed to constrain changes in mica chemistry during magma fractionation and to characterize the relation between the trace-element spectra in mica and geochemical specializations of parental granites. The studied samples covered metaluminous to peralkaline A-type granites of the Madeira pluton (Brazil), metaluminous to peraluminous A-type granites (Kimi, Finland; Orlovka, Russia; Cínovec, Czech Republic) and strongly peraluminous S-type granites (Panasqueira and Argemela, Portugal; Beauvoir, France; Nejdek, Czech Republic). Micas from non-mineralized S- and I-type granitoids from the Czech Republic were analyzed for comparison. For the monitored rare metals, the maximum contents are 1200 ppm Sn (Madeira), 350 ppm W (Beauvoir, Nejdek), 2300 ppm Nb (Madeira) and 200 ppm Ta (Orlovka, Cínovec and Nejdek); Sc reaches maximally 300 ppm at Orlovka. Micas from peraluminous RMG are generally rather enriched in W and Cs, while micas from subaluminous A-type granites are relatively enriched in Nb and Sc. Micas from the studied peralkaline rocks are rich in Nb and poor in Cs, Sc and W. With increasing fractionation of the parental magma, the contents of F, Li, and Rb in mica increase, while the contents of high-field-strength elements (HFSE) usually decrease. This can be attributed to the crystallization of late Li-mica after the HFSE accessories rather than to the effect of the mica crystal structure. Micas affected by high-temperature hydrothermal events are usually completely re-equilibrated. By contrast, low-temperature muscovitization connected with washing out of Li and an increase in Sn affected only rims of mica flakes, leaving crystal cores in their original composition. In a succession from early biotite granites to late Li-mica granites, the share of mica in bulk Sn, Nb and Ta contents in the rocks decreases (50–80 → 5–10%, 10–80 → 1–10% and 100 → <5%, respectively), and rutile, cassiterite and columbite/pyrochlore become the main hosts of rare metals.

1. Introduction

Besides quartz, K-feldspar and Na-dominant plagioclase, micas are the next most abundant rock-forming mineral in rare-metal granites (RMG) of all geochemical types. Due to the specific structure of their crystal lattice, micas usually are the most important carrier of rare alkalis (Li, Rb and Cs) and volatile fluorine, and also an important host of specific high-field-strength elements (HFSE) like Sn, W, Nb and Ta. Moreover, micas are able to concentrate several other elements with conspicuously different chemical properties like Zn and Sc.

A common feature of nearly all mica types in rare-metal granites, their metasomatized varieties (e.g., greisens) and accompanying quartz-dominant lodes is the enrichment in Li: from several hundreds of ppm to about 3 wt% Li, which makes the Li-content of mica the best indicator of

---

[*] Corresponding author at: BIC Brno, Purkyňova 125, CZ-61200, Brno, Czech Republic.
E-mail address: breiter@gli.cas.cz (K. Breiter).

https://doi.org/10.1016/j.lithos.2023.107135
Received 14 October 2022; Received in revised form 13 March 2023; Accepted 14 March 2023

magmatic fractionation of granitic melt. Principles of modern classification of Li-bearing micas were laid already by Foster (1960). The presently valid classification of all micas resulted from long-lasting discussion and is based on the so-called endmembers with several additional names allowed (Rieder, 2001). An overview of our knowledge of micas was published in two volumes of *Reviews in Mineralogy and Geochemistry* edited by Bailey (1984) and Mottana et al. (2002).

In fractionated granites, two different magmatic evolutionary paths of micas can be distinguished: from biotite (i.e., a mixture of annite and siderophyllite) to zinnwaldite, and from muscovite to lepidolite. The third common array of mica compositions forming a line from muscovite across Li-phengite to zinnwaldite is probably a result of hydrothermal alteration.

Mineralogical literature offers a huge number of chemical analyses of micas from granites and pegmatites, mainly using electron microprobe (EMPA), covering major (Si, Ti, Al, Fe, Mn, Mg, Na, K, F) and some minor elements detectable with the microprobe (Rb, Cs, Zn). For a review of older data from granites see Bailey (1984) or Tischendorf et al. (2001), for data from pegmatites see, for example, Černý and Burt (1984) and Černý et al. (2003) and references therein. A common shortcoming of these analyses are the missing contents of Li, an element not detectable with the EMPA. Tindle and Webb (1990) proposed equation allowing to estimate Li contents from the determined contents of Si, of course with a really high uncertainty of the estimated values. In contrast, papers publishing complex chemical analyses of granitic and/or pegmatitic micas, i.e., major elements, Li and trace elements, all performed by local analytical methods with sufficient sensitivity and accuracy, are surprisingly sparse: Van Lichtervelde et al. (2008), Roda-Robles et al. (2012), Xie et al. (2015), Legros et al. (2018), Zhu et al. (2018), Breiter et al. (2017a, 2019a, 2022), Launay et al. (2021) and Monnier et al. (2022). Analyses of major and some trace elements have been published by other authors, but without the determination of Li, which was only estimated (Johan et al., 2012; Li et al., 2015).

As yet, there exists no synoptic study on trace element compositions of micas from rare-metal granites of different geochemical types and grades of differentiation. This paper evaluates a set of about 2600 spot analyses of micas from different types of rare-metal granite plutons made by our team during the last ten years by a combination of electron microprobe and laser-ablation ICP-MS methods. A part of these analyses have already been published within complex studies of specific plutons (Bohemian Massif, Cínovec and Panasqueira deposits, and Argemela granite system – Breiter et al., 2017a, 2019a, 2022, 2023), whereas data from Madeira (Brazil), Beauvoir (France) and Orlovka (Russia) were acquired primarily for this study.

Major goals of this contribution are: (i) to propose a representative dataset of complex chemical analyses of micas from different types of rare-metal granites, (ii) to ascertain chemical differences between micas from different types of fertile magmas, (iii) to describe evolutionary trends in mica chemistry during the differentiation of RMG and following hydrothermal alteration. For these purposes, we focused on the contents of Sn, W, Nb and Ta, rare metals that are currently of great economic interest, and on complementary elements Rb, Cs and Sc, all of which provide important information about magma affiliation and the grade of fractionation.

2. Analytical methods

The contents of major elements in micas were analyzed using the CAMECA SX100 electron microprobe housed at the Institute of Geology of the Czech Academy of Sciences, Praha. Accelerating voltage of 15 kV, a beam current of 10 nA, and a beam diameter of 2 μm were applied. The following standards were used: Na, Al – jadeite, Mg, Si, Ca – diopside, K – leucite, Ti – rutile, Mn – $MnCr_2O_4$, Fe – magnetite, F – fluorite, Rb – RbCl, Cs – polucite, Ba – barite. Counting times on each peak were optimized for individual elements according to their expected concentrations (10–60 s), and half that time was used to obtain background counts. X-ray lines and background offsets were selected to minimize interference. The X-Phi correction procedure (Merlet, 1994) was applied. Chemical analyses of micas were recalculated to the proposed structural formulae based on 44 negative charges. The average detection limits under the operating conditions were as follows: 0.01 wt% for Mg, Ca and Na, 0.02 wt% for Si, Al, Mn, Rb, Cs, K and F, 0.03 wt% for Ti and Zn, and 0.07 wt % for Fe and Ba.

The contents of trace elements in mica samples were analyzed using two different LA-ICP-MS instrumentation setups. The solid-state Nd:YAG laser (UP 213) working at wavelength of 213 nm (New Wave Research, Inc., Fremont, California, USA) was coupled to quadrupole-based ICP mass spectrometer Agilent 7500ce (Agilent Technologies, Inc., Santa Clara, California, USA). This system was installed at the Laboratory of Atomic Spectrochemistry (LAS) of the Department of Chemistry, Masaryk University, Brno. The Nd:YAG laser UP 213 was equipped with an ablation chamber of the type SuperCell™. Aerosol generated in the SuperCell™ was transported by carrier gas (1 l/min He) and mixed with Ar (0.6 l/min) prior to entering the ICP-MS. The sample surface was ablated in the individual spot mode with the following parameters: spot diameter of 50 μm, 10 J/cm^2 fluence, 10 Hz repetition rate, 40 s ablation dwell time and 40 s washout time. The signals of $^{7}Li^{+}$, $^{27}Al^{+}$, $^{28}Si^{+}$, $^{45}Sc^{+}$, $^{69}Ga^{+}$, $^{72,73}Ge^{+}$, $^{93}Nb^{+}$, $^{113,115}In^{+}$, $^{117,118,119}Sn^{+}$, $^{133}Cs^{+}$, $^{181}Ta^{+}$, $^{182,183}W^{+}$, $^{203,205}Tl^{+}$, $^{232}Th^{+}$and $^{238}U^{+}$ were recorded. This instrumentation was used to analyze all the samples from the Bohemian Massif.

The second LA-ICP-MS instrumentation, housed at Faculty of Chemistry, Brno University of Technology and BIC Brno, consists of ArF* excimer laser ablation system Analyte Excite+ (Teledyne CETAC Technologies, Omaha, Nebraska, USA) emitted the laser beam at the wavelength of 193 nm and was connected to quadrupole ICP mass spectrometer Agilent 7900 (Agilent Technologies, Inc., Santa Clara, California, USA). The second laser ablation system Analyte Excite+ has 2-Volume HelEx II Cell and the ablated material was carried using helium carrier gas (0.5 + 0.3 l/min) and mixed with argon (~1 l/min) prior to the torch. The sample surface of individual spots was ablated by a 50 μm laser beam diameter with a fluence of 3 J/cm^2 and a repetition rate of 10 Hz. Each spot analysis incorporates 40 s background (Ar-He gas blank) followed by 35 s of data acquisition from the sample. The monitored isotopes were as follows: $^{7}Li^{+}$, $^{27}Al^{+}$, $^{28}Si^{+}$, $^{39}K^{+}$, $^{45}Sc^{+}$, $^{47,49}Ti^{+}$, $^{55}Mn^{+}$, $^{56,57}Fe^{+}$, $^{69}Ga^{+}$, $^{72,73}Ge^{+}$, $^{85}Rb^{+}$, $^{93}Nb^{+}$, $^{113,115}In^{+}$, $^{116,117,118,119}Sn^{+}$, $^{133}Cs^{+}$, $^{181}Ta^{+}$, $^{182,183}W^{+}$, $^{203,205}Tl^{+}$, $^{232}Th^{+}$, $^{238}U^{+}$. This instrumentation was used to analyze samples from Madeira, Kimi, Orlovka, Argemela, Panasqueira and Beauvoir granites.

In the case of several elements (Ti, Fe, Ge, In, Sn, W and Tl), two or more isotopes were measured to identify and exclude the presence of possible spectral interferences. Limits of detection were calculated as $3 \times SD / b$ where SD means standard deviation of He-Ar gas blank and b is the sensitivity. The average detection limits under the operating conditions were as follows: 1.8 ppm Li; 1.5 ppm Al, 170 ppm Si, 0.70 ppm Sc, 0.18 ppm Ga, 1.0 ppm Ge, 0.08 ppm Nb, 0.04 ppm In, 2.1 ppm Sn, 0.15 ppm Cs, 0.08 ppm Ta, 0.21 ppm W, 0.41 ppm Tl, 0.01 ppm Th, and 0.01 ppm U in the case of UP 213 coupled to Agilent 7500ce, and 1.7 ppm Li, 7.1 ppm Al, 440 ppm Si, 13 ppm K, 0.23 ppm Sc, 0.63 ppm Ti, 0.41 ppm Mn, 1.8 ppm Fe, 0.02 ppm Ga, 0.28 ppm Ge, 0.32 ppm Rb, 0.01 ppm Nb, 0.08 ppm In, 0.13 ppm Sn, 0.02 ppm Cs, 0.01 ppm Ta, 0.01 ppm W, 0.02 ppm Tl, 0.01 ppm Th, and 0.01 ppm U in the case of Analyte Excite+ coupled with Agilent 7900.

Accuracy control when using both the above-mentioned instrumentations was performed by repeated measurements of the mica in-house test sample measured together with all the samples included in this publication.

Both ICP mass spectrometers were tuned using SRM NIST 612 with respect to the maximum sensitivity, and minimum doubly charged ions, oxide formations ($^{248}ThO^{+}/^{232}Th^{+} < 1\%$) and mass response $^{238}U^{+}/^{232}Th^{+} \sim 1$. The potential polyatomic interferences were minimized via a collision cell (He 1 ml/min) in both cases. The elemental contents were calibrated using artificial glass standards SRM NIST 610 and 612, and Si and Al as internal reference elements after baseline correction and integration of the peak area using Grams/AI Spectroscopy Software (Thermo Scientific™, Bremen, Germany) and HDIP software (Teledyne CETAC Technologies, Omaha, Nebraska, USA).

3. Methods of data presentation

The results of EMPA and LA-ICP-MS analyses of micas are given in Tables 1–13 (in Electronic Appendix) as medians of particular parental rock types. The Fe/Mg ratio is calculated as the Fe/(Mg + Fe)*100 atomic value and signed as (#Fe). This means that annite has #Fe > 50, while phlogopite has #Fe < 50 (all in atoms per formula unit, apfu).

Figs. 4–11 were constructed exclusively from data acquired by the authors using the above described methods. As Li is a reliable indicator of mica evolution during magma fractionation (Černý et al., 1985), Li contents were used as the main parameter to present evolutionary trends of all other discussed elements graphically.

Mica mineral names follow IMA rules (endmembers) with additional names allowed (Rieder, 2001): biotite = a mixture of annite, phlogopite and siderophyllite; lepidolite = a mixture of trilithionite and polylithionite; phengite = Fe-bearing muscovite; zinnwaldite = mica in ideal center of the Li –R^{3+} – R^{2+} ternary diagram, i.e., an intersection of the Sid–Pln and Ann–Tln joins. Mineral symbols follow the recommendations by Warr (2021); "Phg" is used for phengite.

4. Geology of the studied granites and major-element characteristics of their micas

In the text below, we divided rare-metal granites into three geochemical types because different chemical properties of parental magmas are decisive for the chemical compositions of micas and their evolution during magma differentiation. Among several chemical classifications of granitoids with geotectonic connotations, the "alphabet" classification involving A-, I-, S- (M-, C-) types has been widely accepted, but also criticized (Frost et al., 2007). Another geotectonically oriented granite classification was proposed by Pearce et al. (1984). Classification based of phosphorus content, especially for RMGs, was proposed by Taylor and Fallick (1997). None of the mentioned concepts gained universal support; among several summarizing papers, Bonin (2007) gives a good overview.

The classification of strongly peraluminous and phosphorus-rich (sensu Taylor and Fallick, 1997) orogenic granites with dominantly metasedimentary sources as "S-type granites", and the classification of mostly subaluminous orogenic granites with dominantly meta-igneous sources as I-types (Chappell and White, 1974) is generally accepted. By contrast, the use of the designation "A-type granites" (Loiselle and Wones, 1979) remains slightly controversial: some authors stressed the chemical peculiarities of this rock group (Whalen et al., 1987), other stressed its rift-related origin (Haapala et al., 2007) or its up to peralkaline character (Goodenough et al., 2000) of some plutons or their parts. It is a problem that these approaches are not in a desirable correlation. Therefore, Eby (1992) distinguished two different sources of A-type magmas: A1 formed in oceanic islands and along continental rifts, and A2 formed particularly in the deeper crust. The subject is even more complicated when fractionated late facies of plutons are discussed because shift from sub- to peraluminous, a shift from WPG to COLG (Pearce et al., 1984) and a shift from A2 to A1 fields (Eby, 1992) of the classification schemes during fractionation is common (due to Rb, Nb etc. enrichment vs. Y, Yb depletion during the fractionation).

Nevertheless, the existence of a specific type of granites with typical chemical features (mostly only slightly peraluminous, with very low contents of phosphorus during the whole suite evolution, relative high contents of HFSE, flat REE distribution patterns, high Fe/Mg values etc.), emplaced in a tensional setting (anorogenic, post-orogenic) and often related to rhyolitic volcanism is a fact (Dall'Agnol et al., 2012; Frost et al., 2007; Martin, 2006 and references therein). These suites usually started as metaluminous, often rapakivi-textured granites (Wiborg batholith, Amazon craton), while their late phases change mostly to peraluminous composition (Kimi and Eurajoki in Finland, Haapala, 1995; Água Boa pluton in Amazon, Borges et al., 2009), sometimes to peralkaline composition (Madeira and Europa plutons in Amazon, Costi et al., 2009). Others are related to post-orogenic extension with rhyolite volcanism (Cínovec, this paper; topaz rhyolites in the SW of U.S.A., Christiansen et al., 2007). Granites of this group meet most of the chemical features defined by Loiselle and Wones (1979), lie in the "WPG" and partly "COLG" fields of Pearce et al. (1984), are "low-phosphorus" according to Taylor and Fallick (1997), their less evolved facies fall in A2 field according to Eby (1992), and display high Fe/Mg values etc. (Fig. 1). These granites are usually termed as "A-type granites" in the last two decades. We use this term together with dozens of other authors studying rare-metal granites (Dall'Agnol et al., 2012 and references therein). From practical point of view, we divided the A-type rocks to two subgroups: those evolving from metaluminous to peraluminous compositions (Kimi, Cínovec, Orlovka), and those evolving from metaluminous to peralkaline compositions (Madeira).

4.1. *Metaluminous to peralkaline A-type granites*

4.1.1. *Madeira pluton, Pitinga magmatic province, Brazil*

The Pitinga magmatic province (1824–1818 Ma), composed of Madeira, Agua Boa and Europa A-type plutons, is situated in the central part of the Amazon craton, Brazil (0.754°S, 60.106°W, Costi et al., 2009), intruding the 1889–1888 Ma Iricoumé Group volcanic basement.

The Madeira pluton (60 km^2) consists of four principal rock types (Bastos Neto et al., 2009; Costi et al., 2000): (i) metaluminous porphyritic amphibole-biotite "rapakivi granite" (1824 ± 2 Ma), (ii) metaluminous biotite granite (1822 ± 2 Ma), (iii) a sheet-like body of metaluminous hypersolvus alkali feldspar granite, and (iv) the central body of F, Sn, Th and Zr-rich albite granite in two facies. The magmatic "core facies" is chemically peralkaline and enriched in disseminated cryolite, cassiterite, zircon, pyrochlore, and thorite, and contains two major zones of veins and pockets mainly composed of cryolite, besides layers of intragranitic cryolite-rich pegmatites (Paludo et al., 2018). The outer shell of the albite granite, the "border facies", underwent pervasive hydrothermal alteration: it is now slightly peraluminous, very poor in mica, and contains common fluorite instead of cryolite. The latest two granites are interpreted as coeval, with the age of 1818 ± 2 Ma (Costi et al., 2000, 2009).

Micas from six representative samples (140 spots, Table 1) of all granite types of the Madeira pluton were analyzed for this study. The studied micas correspond to nearly ideal annite in the rapakivi-type granite, to biotite to siderophyllite, partly altered to phengite in the biotite granite, Li-enriched annite in the hypersolvus granite, and intergrowths of Zn, Rb-rich annite and Rb, Zn-rich lepidolite in the peralkaline core facies of the albite granite (Fig. 2a, 3a). A specific features of micas from the core albite granite are their association with riebeckite and cryolite, and rather unusually high contents of Zn of up to 1.1 apfu Zn in annite (8.94 wt% ZnO, Fig. 3e, f) and up to 0.5 apfu Rb in lepidolite (up to 5.48 wt% Rb_2O, Costi et al., 2009). Content of fluorine reaches 3.5 apfu F in the lepidolite being substantially lower in all other mica types.

4.2. *Metaluminous to peraluminous A-type granites*

4.2.1. *Wiborg batholith and Kimi stock, Finland*

The Wiborg batholith (1.67–1.54 Ga) intruding the Paleoproterozoic Svecofennian basement (1.9–1.8 Ga) of southern Finland is dominantly composed of wiborgite. The most evolved part of the batholith, the Kimi stock is zoned and composed of medium-grained porphyritic biotite granite in the center, medium-grained equigranular Li-mica-topaz granite at the margin and marginal pegmatite (stockscheider) along the stock contact (Lukkari et al., 2009).

Micas from four typical rock samples (85 spots, Table 2, Fig. 2b) were

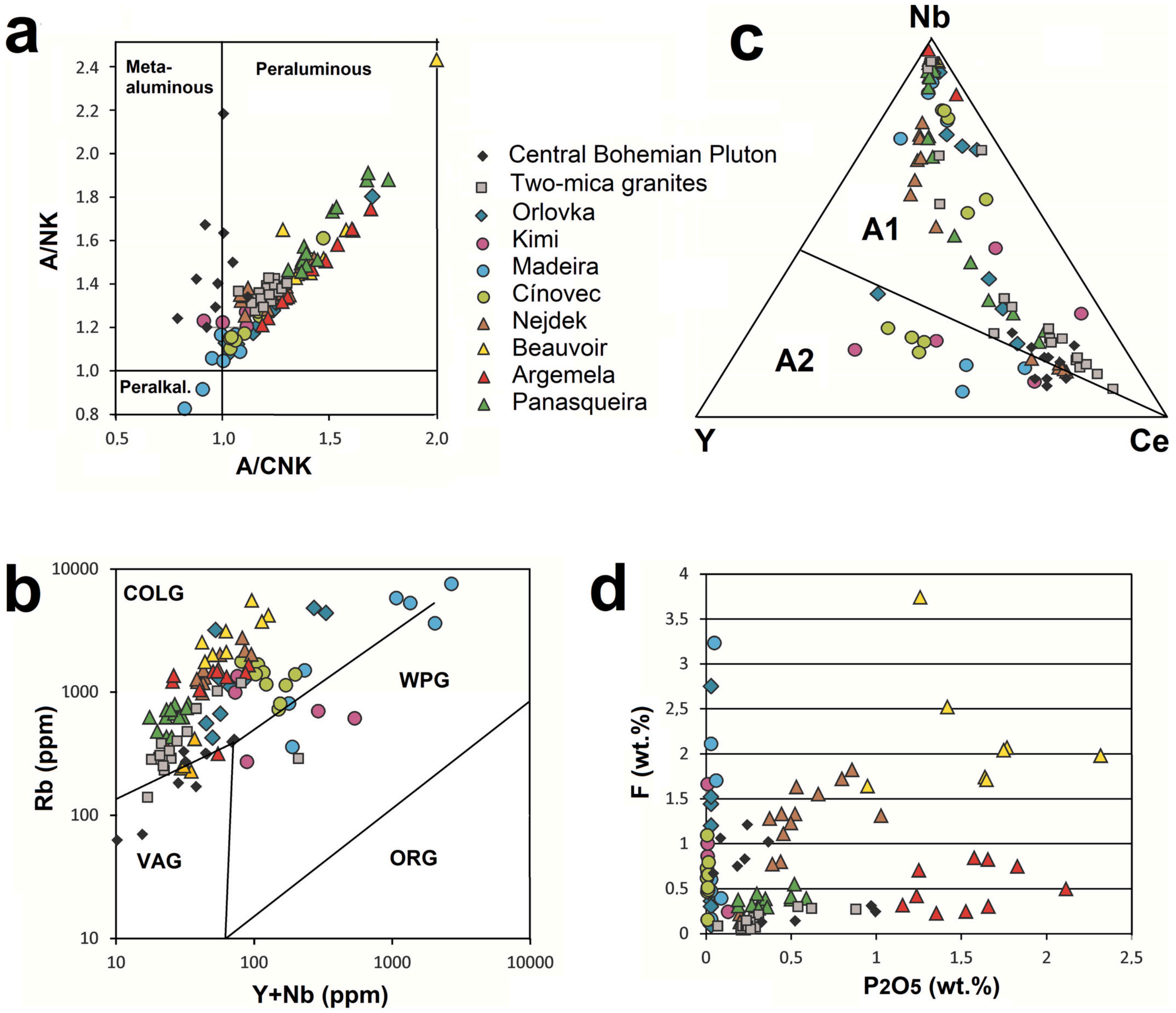

Fig. 1. Granite classification diagrams: position of studied granite suites in classification schemes according to: a, Shand (1943); b, Pearce et al. (1984); c, Eby (1992); d, Taylor and Fallick (1997).

analyzed for this study. Mica from the rapakivi granite is Fe-rich biotite (annite), while mica from the Kimi stock is classified as siderophyllite. Mica from the stockscheider occupies a rather unusual position in the theoretical solid solution gap (Monier and Robert, 1986) among siderophyllite, zinnwaldite and muscovite, which probably indicates a strong hydrothermal alteration. The contents of F and Li in micas from wiborgite are very low, and only moderately enriched in rocks from the Kimi stock.

4.2.2. A-type granites in the Eastern Erzgebirge and the Cínovec Sn-W-Li deposit

Granites of the Krušné hory/Erzgebirge have been, for their obvious association with tin mineralization, investigated in detail petrographically and chemically since the mid-19th century and belong to one of the classical regions of ore-bearing granites in the world (Breiter et al., 1999). Alongside the prevailing strongly peraluminous phosphorus-rich granite plutons of S-type in the western part of the area (see the following chapter on the Nejdek pluton), smaller stocks and one volcanoplutonic complex of subaluminous P-poor granitoids of A-type geochemical signature dominate in its eastern part (Breiter, 2012).

The Altenberg-Teplice Caldera is the largest complex of A-type rhyolites and granites in Variscan Europe, covering about 500 km^2, 314–313 Ma in age (Tichomirowa et al., 2022). In an extensional tectonic regime after the caldera collapse, small plutons of A-type biotite granites intruded the rhyolite sheet. The intrusions of biotite granites were followed by the emplacement of a number of cupolas and small subvolcanic stocks and explosive pipes (Seltmann and Schilka, 1991) of albite-zinnwaldite-topaz granites with tin mineralization. The Cínovec/Zinnwald cupola is well known due to borehole CS-1, 1596 m in depth (50.7332°N, 13.7653°E) providing unique material for petrological study. The deeper part of the granite body, below the depth of 736 m, is formed by different facies of metaluminous albite-biotite granites, while the upper part is formed by mostly peraluminous albite-zinnwaldite granite. The uppermost part of the granite cupola is greisenized and mineralized with cassiterite and wolframite (Breiter et al., 2017b; Johan et al., 2012).

Mica from 41 samples (>900 spots, Tables 3–5) from the whole borehole CS-1 and mineralized rocks of the Cínovec deposits were

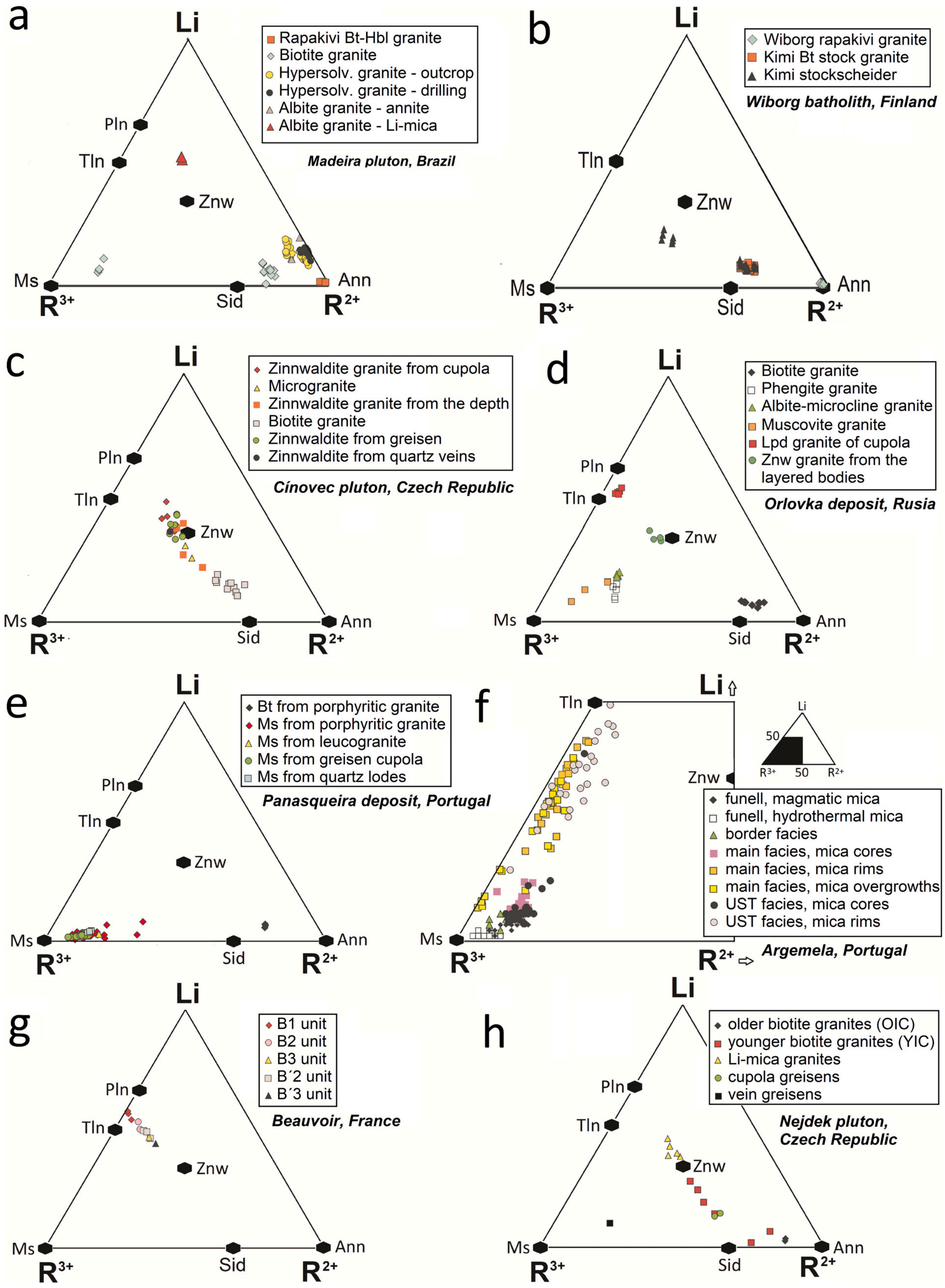

Fig. 2. Micas classification according to Foster (1960): a, Madeira; b, Kimi; c, Cínovec; d, Orlovka; e, Panasqueira; f, Argemela; g, Beauvoir; h, Nejdek.

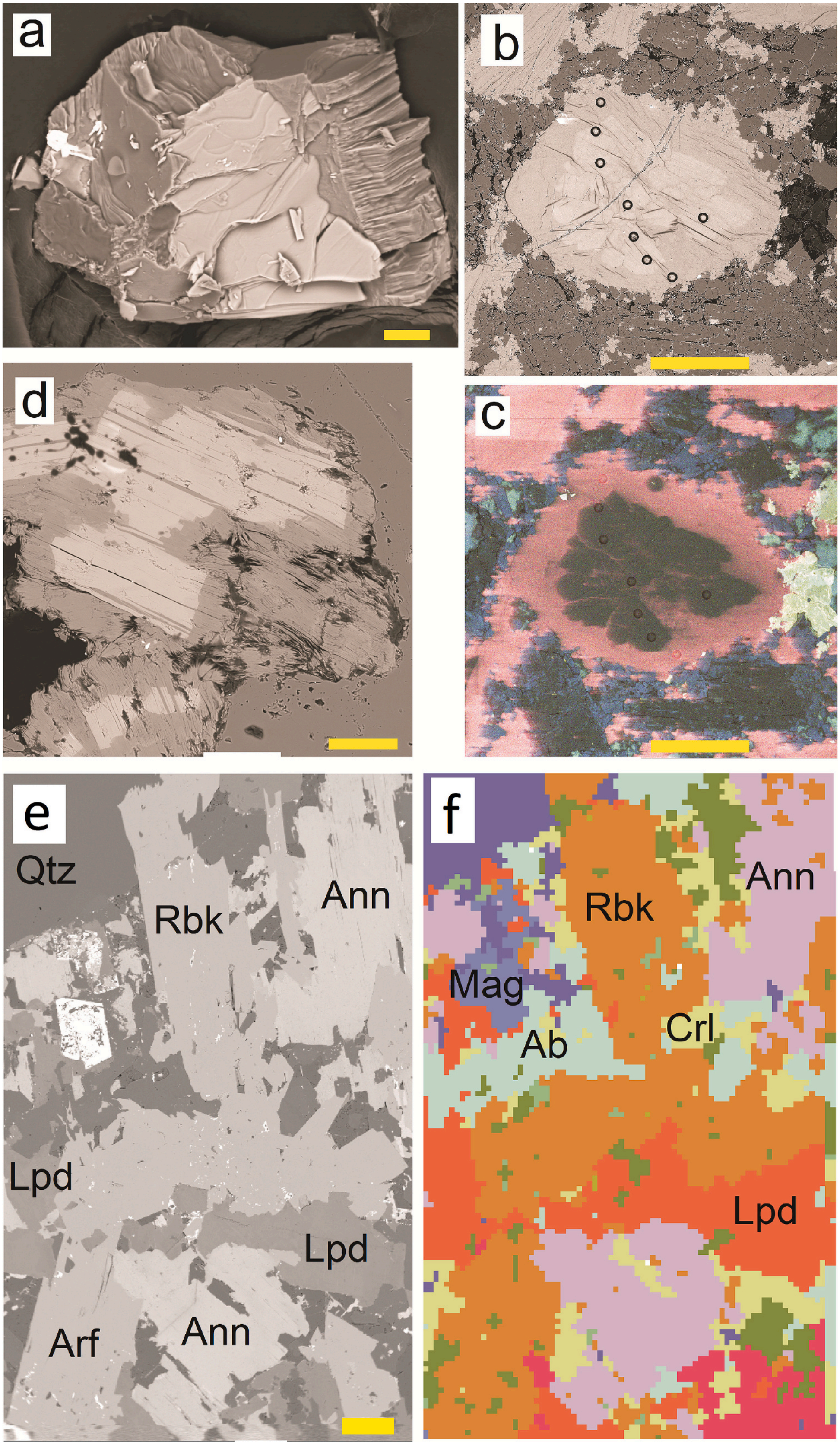

Fig. 3. Some unusual mica textures: a, BSE image of zoned mica grain from the Madeira albite granite: core of Zn, Rb-rich annite (light) surrounded by Zn, Rb-rich lepidolite (dark), scale bar 25 µm; b, BSE image of zoned mica phenocryst from the porphyritic granite facies at Argemela: early magmatic core of phengitic muscovite (light) rimmed by late magmatic lepidolite (dark), scale bar 500 µm; c, CL image of previous mica grain: the Mn-bearing lepidolite rim shows intensive magenta CL, scale bar 500 µm; d, late muscovitization of zinnwaldite in greisen, Cínovec deposit: core of residual zinnwaldite (light) surrounded by metasomatic Sn-enriched phengitic muscovite (dark), scale bar 100 µm; e, BSE-image of detail annite–lepidolite–arfvedsonite intergrowths from the Madeira albite granite, scale bar 100 µm; f, TIMA mineral map (Hrstka et al., 2018) of the area of previous image. (For interpretation of the references to colour in this figure legend, the reader is referred to the web version of this article.)

studied in detail by Breiter et al. (2019a). Mica from the "biotite granite" should be correctly termed Li-enriched siderophyllite, while mica from the zinnwaldite granite and greisen is true zinnwaldite (Fig. 2c). [Remember that the mineral zinnwaldite was first described from this place and named after the German variety of the name of this deposit.] Note that all analyses form an array pointing from siderophyllite in the direction to polylithionite. The contents of F are high in all types of referred micas, evolving from ca. 4 wt% in "biotites" to 8.5 wt% (3.85 apfu F), i.e., nearly full F occupancy of the OH-F sites, in zinnwaldite. Moreover, Li increases from ca. 1 wt% to max. 5.3 wt% Li_2O, i.e., 3 apfu Li.

4.2.3. Khangilai granite pluton with the Orlovka Ta-deposit, Transbaikalia, Russia

The Khangilai pluton, Jurassic in age, is highly fractionated, only slightly peraluminous A-type magmatic system located 140 km SE of the city of Chita (51.055°N, 114.834°E). While the central part of the pluton is formed by barren biotite and two-mica granites, the layered cupola-like body of the western satellite (hereafter Orlovka deposit) is mineralized with Ta (Badanina et al., 2004; Breiter et al., 2019b). The layered sequence is generally composed of: (i) biotite granites, (ii) granites with phengite as the major mica, and (iii) Li-mica granites. Altogether 150 spots were analyzed (Table 6). The classification of micas from Orlovka follows the aforementioned rock division. Biotite granites contain Fe > Mg mica near the ideal siderophyllite composition (Fig. 2d). Micas of the muscovite–phengite group form an array trending from ideal Ms. to ideal Znw, however, not occupying the end member positions but having mostly Li-enriched "phengitic" compositions. An increase in Fe, Li and F is positively well correlated. Micas from the cupola fit nearly ideal lepidolite in their composition, while the geologically youngest rocks – banded aplites to pegmatites – contain nearly ideal zinnwaldite.

4.3. Strongly peraluminous granites

4.3.1. Panasqueira granite pluton and associated W deposit, Portugal

The Panasqueira W deposit is located 25 km SW of the city of Covilha in central-eastern Portugal (40.156°N, 7.755°W). Here, late Variscan peraluminous granites form a completely hidden pluton intruding the Cambrian Beira schists, known only from mining operations and exploration boreholes (Breiter et al., 2023). The pluton consists of outer porphyritic two-mica granite and central, more evolved muscovite leucogranite forming a cupola. Both granites are peraluminous. The uppermost part of the cupola was transformed to quartz-rich greisen, but the world-class W (+Sn, Cu) deposit appears as a flat sheet of quartz lodes richly mineralized with coarse-grained wolframite (Marignac et al., 2020). Altogether 200 spots were analyzed in 9 representative samples.

Porphyritic granite contains biotite close to the siderophyllite end-member, together with prevailing Mg, Fe slightly enriched muscovite-phengite. Compared to typical rare-metal granites, both micas are poor in Li (<0.5 wt% Li_2O) and F (<2 wt% F). The compositions of dioctahedral micas from leucogranite, greisen and quartz veins are close to ideal muscovite (Table 7, Fig. 2e, compare also Launay et al., 2021).

4.3.2. Argemela granite stock, Portugal

The Argemela leucogranite intrusion is exposed as a small rounded body hosted by weakly metamorphosed schists of the Beira series of Upper Cambrian age about 8 km west of the Fundão town, central-eastern Portugal (40.155°N, 7.604°W). A predominant part of the outcrop is formed by porphyritic fine-grained leucogranite, while <5% of the outcrop are formed by equigranular, fine-grained granite. A layered zone 0.4–1 m thick, locally combined with unidirectional solidification textures, evolved along the contact of the porphyritic and the equigranular facies. Several dikes of fine-grained leucogranite or aplite were found to crosscut the schists near the granite stock and supposed to be a feeder channel for the Argemela granite (Charoy and Noronha, 1996).

Micas from Argemela were already studied by Charoy and Noronha (1996), Michaud and Pichavant (2020) and Breiter et al. (2022). For this review, 184 spots in 8 samples from Breiter et al. (2022) were evaluated (Table 8). All mica types from Argemela are dioctahedral members of the muscovite–phengite–lepidolite series (Fig. 2f). Subhedral–euhedral mica flakes 0.5–2 mm in size in the porphyritic facies and the layered zone are composed of three distinct zones: (i) early magmatic euhedral to subhedral Li-phengitic cores, (ii) late magmatic subhedral lepidolite rims, and (iii) hydrothermal irregular overgrowths of fine-grained lepidolite or muscovite (Fig. 3b, c). Mica from the equigranular facies is homogeneous and should be classified as Li-enriched phengite (1.5–3.0 wt% FeO, 0.3–0.5 wt% Li_2O), while mica from the funnel facies shows a distinct zoning: subhedral magmatic cores are composed of Li-enriched phengite (1.5–3.0 wt% FeO, ca. 0.25 wt% Li_2O), while the anhedral hydrothermal overgrowths are composed of nearly pure muscovite (0.1 wt% Li_2O, <1 wt% FeO).

4.3.3. Beauvoir granite, France

The Beauvoir granite forms a small body (<0.2 km^2) at the southern edge of the late Variscan Echassières granite pluton in the northern part of the Massif Central, France (46.179°N, 2.953°E). Geochemically it is a highly specialized, strongly peraluminous (ASI = 1.3–1.4), rare metal-bearing granite. Borehole GPF1, 900 m deep, allowed to study the vertical evolution of the Beauvoir granite along a section over 700 m long. Cuney et al. (1992) described vertical zoning of the stock and defined three units with increasing grade of magmatic fractionation from B3 at the bottom to B1 at the top of the body. Somewhat later, Raimbault et al. (1995) subdivided the Beauvoir granite into two major units: the B-unit builds the upper part of the stock, representing a geochemically more evolved, more fluid-enriched part of the Beauvoir initial magma, while the B´-unit, smaller in volume, represents a relatively less evolved and later emplaced portion of the Beauvoir magma. Separation of the B- and B´melts occurred at the early stage of the granite system evolution. Later, the two melts in fact fractionated independently. Thus, the upper B-unit can be divided into three sub-units, from the uppermost ultimately fractionated B1-unit (at a depth of 98–423 m) through the B2-unit (at a depth of ca. 423–571 m) to the B3-unit (at a depth of 765–790 m). Within the lower B´-unit, the relatively more fractionated B´2-unit (at a depth of ca 571–746 m) and the less fractionated B´3-unit (at a depth of ca. 850–870 m) can be distinguished. For our review, the model by Raimbault et al. (1995) was accepted.

Vertical variations in the composition of mica from zinnwaldite in B3 to lepidolite in B1, well illustrating changes in the bulk chemical composition of granite, was already reported by Monier et al. (1987) using microprobe and wet chemistry. Trace element compositions of micas from granite and associated greisen and quartz veins were recently reported by Monnier et al. (2022) by LA-ICP-MS.

We analyzed 10 samples of mica from fresh granite along borehole GPF-1 to monitor its vertical evolution (230 spot analyses, Table 9). Mica in the whole Beauvoir profile is rich in Li and Rb, evolving from Li-rich zinnwaldite in unit B´3 to ideal lepidolite (i.e., a mixture of trilithionite and polylithionite in a ratio close to 1:1) in unit B1 (Fig. 2g). The contents of FeO and MnO decrease from units B´3 and B3 to unit B1 (7.5 → 0.6 wt% FeO, 1.3 → 0.15 wt% MnO), while Li, F and Rb increase in the same direction (4.5 → 6.5 wt% Li_2O, 1.1 → 1.8 wt% Rb_2O, 7.2 → 8.5 wt% F). The Mn/Fe value increases with fractionation, being clearly higher in the B-units (Mn/Fe = mostly 0.2 and higher) than in the B´-units (Mn/Fe = 0.125–0.17).

4.3.4. Nejdek pluton and Sn-W mineralization

The Nejdek pluton, including the late, highly fractionated Podlesí stock, is the most typical example of a strongly peraluminous rare-metal granite pluton in the western Krušné Hory/Erzgebirge area (Breiter et al., 1999). This pluton is composed of an older intrusive suite of barren biotite granites, 328.6 ± 2 Ma in age and a younger intrusive suite of ore-productive albite-biotite granites with topaz (319.8 ± 1 Ma, Tichomirowa and Leonhardt, 2010). The most highly fractionated, extremely F- and P-rich batches of residual magma crystallized at Podlesí (50.4327°N, 12.7754°E) in the form of a small stock of albite-zinnwaldite-topaz granite with additional flat dikes with magmatic layering (Breiter et al., 2005).

Pericontact quartz-muscovite greisens with wolframite mineralization evolved in some of the cupola-like structures of medium-grade fractionated topaz-biotite granites, while steep vein-like quartz-muscovite (±topaz, apatite, tourmaline) greisens mineralized with cassiterite were found in deeply eroded parts of the pluton.

For the purpose of this review, about 350 spot analyses from 16 samples are available (Tables 10, 11). Micas from the older intrusive suite are biotite (a mixture of annite and siderophyllite), while micas in the younger suite evolved from annite-siderophyllite to zinnwaldite (Fig. 2h). These igneous micas are generally homogeneous. Micas from the greisen are hydrothermally altered and rather patchily inhomogeneous. They should be classified as Li-enriched biotite in cupola-seated greisens and as Li-phengite in vein-type greisens.

4.4. *Common granites for comparison*

4.4.1. *Central Bohemian I-type pluton (CBP), Czech Republic*

The Central Bohemian pluton, situated in the south-central part of the Czech Republic, is a composite pluton, comprising intrusive suites of different geochemical types (354–336 Ma, Holub et al., 1997). The most important suites are: (i) the calc-alkaline Sázava suite – mostly metaluminous amphibole-biotite tonalites and quartz diorites to biotite trondhjemites and granodiorites with associated basic rocks; (ii) the high-K calc-alkaline Blatná suite – biotite ± amphibole granodiorites and granites and associated shoshonitic basic rocks; (iii) the highly K- and Mg-enriched Čertovo Břemeno suite, containing porphyritic amphibole-biotite melasyenites and melagranites (durbachites), biotite-two-pyroxene melasyenites, and associated K- and Mg-rich (amphibole)-biotite granites; and (iv) the peraluminous Říčany suite – biotite (±muscovite) granites. Five studied samples represent the four above mentioned suites; 110 mica analyses are available.

All trioctahedral micas are classified as biotite (Table 12): in the case of tonalite of the Sázava suite and granodiorites of the Blatná suite they correspond to annite (#Fe = 51–57), while in the peraluminous Říčany granite and in the high-K, -Mg (durbachite-like) suite they correspond to phlogopite (#Fe = 0.41–0.42). The contents of F and Li in all referred micas are negligible, reaching max. 0.2 wt% Li_2O and 0.6 wt% F in the Říčany granite.

4.4.2. *Peraluminous granites of the South Bohemian batholith, Czech Republic/Austria/Bavaria*

The South Bohemian batholith is a complex of Variscan granites intruding the Moldanubicum crystalline unit (330–315 Ma, Gerdes et al., 2003). It can be divided into the eastern branch in southern Bohemia and northern Austria (Waldviertel) and the western branch in western Bohemia and NE Bavaria (Böhmerwald, Oberpfalz). It is composed of numerous composite bodies of several texturally and mineralogically distinct granite types, especially Weinsberg biotite granite, Freistadt biotite granodiorite, Eisgarn two-mica granite etc. (Finger and Clemens, 2002). A typical facies of strongly peraluminous two-mica granites, traditionally termed as Eisgarn type, was selected for the present study. The studied samples slightly differ in their textures and chemical compositions: 4 samples of Eisgarn s.s. granite from the Central Moldanubian pluton (CMP) in the SE (48.92°N, 15.10°E, Breiter and Koller, 1999), 3 samples from the Plechý/Plöckenstein pluton (PPP) in the S (48.77°N, 13.84°E, Breiter et al., 2007) and 3 samples from the Rozvadov pluton in the western part of the batholith (49.75°N, 12.40°E, Siebel et al., 2008). All these rocks are interpreted as products of voluminous melting of the surrounding Moldanubian basement during, and shortly after, the thermal peak of the Variscan orogeny (Gerdes et al., 2003). Muscovite is interpreted as a primary magmatic mineral in all studied granites (Breiter and Koller, 1999). It is partly replaced by sillimanite in the deformed facies.

Samples from all these plutons allow comparing chemical compositions of associated biotites and muscovites. All "biotites" hold a substantial proportion of the siderophyllite component, differing in the #Fe value (#Fe = 42–84). Associated muscovites are chemically rather homogeneous, near the ideal endmember. Both biotites and muscovites are poor in Li (max. 0.5 wt% Li_2O). The contents of F in muscovites are mostly <0.5 wt%, and those in biotites are mostly below the detection limit of EMPA.

4.4.3. *Mafic micaceous rock (Glimmerite)*

Several dikes of extremely Mg-rich mafic rock composed of plagioclase and phlogopite with only subordinate K-feldspar and quartz (49.5–51.3 wt% SiO_2, 14.0–17.1 wt% MgO) crosscut the Moldanubian crystalline rocks near the town of Prachatice, southern Bohemia (48.94°N, 14.05°E, Breiter and Koller, 2009). Two samples (50 spots) were analyzed as examples of mica crystallized from ultramafic magma.

These trioctahedral micas have a composition of phlogopite (#Fe = 19–22, Table 12) with negligible contents of F and Li.

4.4.4. *Durbachites*

Melanocratic K- and Mg-enriched granitoids (durbachites) represent one of typical components of the European Variscan orogeny. The Třebíč pluton is the largest (49.215 N, 15.88E, 160 km^2, Holub, 1997) of the several durbachitic intrusions in the Moldanubian unit of the Bohemian Massif. Two samples (46 spots) represent the coarse- and medium-grained facies of amphibole-biotite melasyenite, the most typical rocks of the whole durbachitic series. Micas from durbachites are phlogopites (#Fe = 33) with low contents of F (~0.2 wt%) and Li (~0.02 wt% Li_2O) (Table 12).

5. Contents of minor and trace elements in micas

5.1. *Lithium*

Micas are the most common carrier of Li in all types of granites. Other Li minerals like amblygonite ($LiAlPO_4F$), spodumene ($LiAlSi_2O_6$), petalite ($LiAlSi_4O_{10}$), Li-Fe-Mn-phosphates and Li-tourmalines are specific of pegmatites and appear only rarely in granites.

Among the studied samples, the contents of Li in trioctahedral micas varied from tenths of ppm in phlogopite from ultramatic rocks (glimmerites) through hundreds of ppm in biotites from common I-type granites (Central Bohemian pluton), 1000–2000 ppm in biotites from common S-type granites (South Bohemian Batholith) up to about 20,000 ppm in zinnwaldites from fractionated RMG (Cínovec) and 30,000–34,000 ppm in lepidolite from the most fractionated leucocratic RMGs (Beauvoir), i.e. reaching the theoretical maximum of Li contents in mica. About 2000 ppm Li were found in dioctahedral muscovite from common S-type granites and 10,000–20,000 ppm Li in muscovites crossing the di−/tri-octahedral transition at Argemela.

The contents of Li well positively correlate with F and Rb contents, which is caused by similar behavior of all these elements in fractionated granitic melt, not by relations in mica crystal structure. The Li enrichment in mica well correlates with Li enrichment in fractionating granitic melt without any relation to its geochemical type or grade of peraluminity/alkalinity. Generally, Li-enrichment in mica is a typical feature of most rare-metal granites.

5.2. *Rare metals Sn, W, Nb and Ta*

Rare metals as Sn, W, Nb and Ta are typical high-field-strength-elements (HFSE) with a strong tendency to enter Ti oxides or form relatively early crystallized oxide minerals like rutile, cassiterite, and columbite or pyrochlore groups of minerals. The contents of these elements in mica thus depend on the timing of crystallization of mica vs. that of the accessory minerals, and of course, on later fluid-related processes.

Tin is one of the ubiquitous trace elements in micas: even phlogopites and biotites from geochemically primitive I-type tonalities, granodiorites and associated rocks in the Bohemian Massif contain 30–120 ppm Sn (Fig. 4f). Of course, Sn contents in micas from rare metal granites reach much higher values: up to 1300 ppm Sn were found in annite from albite granite from Madeira pluton and up to 600–800 ppm in biotites from Orlovka, Cínovec, Panasqueira, Argemela and Nejdek plutons (Fig. 4).

The behavior of Sn in micas during the evolution of the plutons is highly variable. It seems that the Sn contents in micas gradually increase during the evolution of slightly to moderately fractionated pluton facies (i.e., Sn positively correlates with Li), while Sn usually decreases in the final stage of fractionation of rare-metal granite plutons, as observed at Cínovec and Nejdek (Figs. 4c, e). In contrast at Madeira pluton, the Sn contents reaches its maximum in annite from the youngest peralkaline

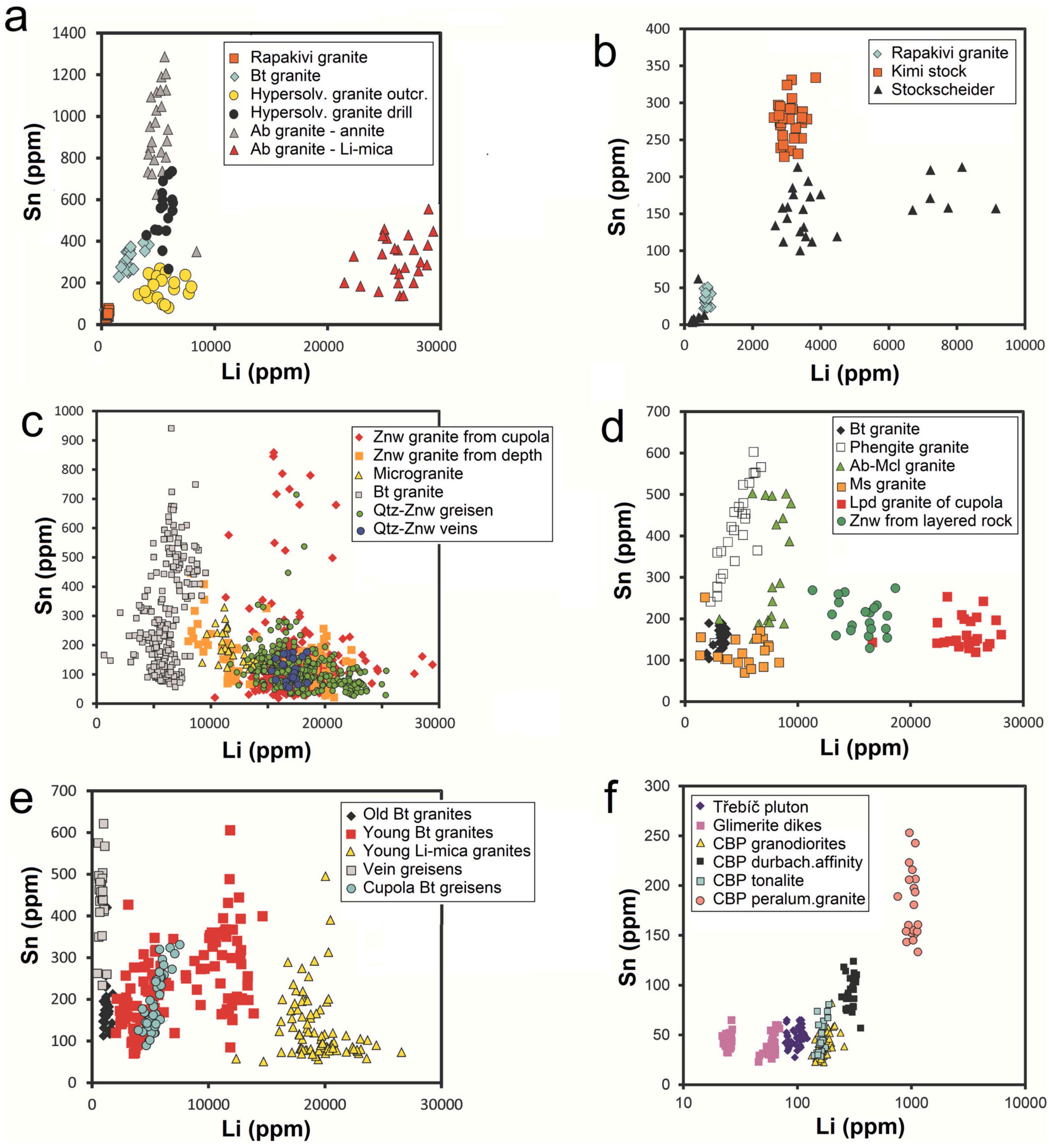

Fig. 4. Variation in Sn-contents in micas from selected granite plutons: a, Madeira; b, Kimi; c, Cínovec; d, Orlovka; e, Nejdek; f, primitive granitoids.

albite granite, nevertheless associated lepidolite is relatively Sn-poor (Fig. 4a). At Orlovka (Fig. 4d), the interpretation is difficult as phengite and muscovite are also present besides Fe-Li micas. In common two-mica granites, muscovite is usually slightly Sn-enriched compared to associated biotite (Koller and Breiter, 2003).

The dispersion of Sn contents in a particular rock type is wide, especially in biotite (Figs. 4c, d), which obscures any discussion about the correlation among associated elements. Micas from Beauvoir are specific in containing 100–400 ppm Sn in all evolutionary stages of this pluton, with no correlation with Li or other elements. The behavior of Sn during greisenization is also variable. While the Sn contents in zinnwaldite from greisen at Cínovec equal those in the ambient granites (<250 ppm Sn), muscovite-phengite from vein greisens in the Nejdek pluton are Sn-enriched compared to the surrounding granite (450 vs. 107 ppm Sn). Strong Sn-enrichment of secondary muscovite was observed also in relative scarce greisens at Beauvoir (Monnier et al., 2022).

Tungsten, although usually accompanying tin in the so-called Sn-W-

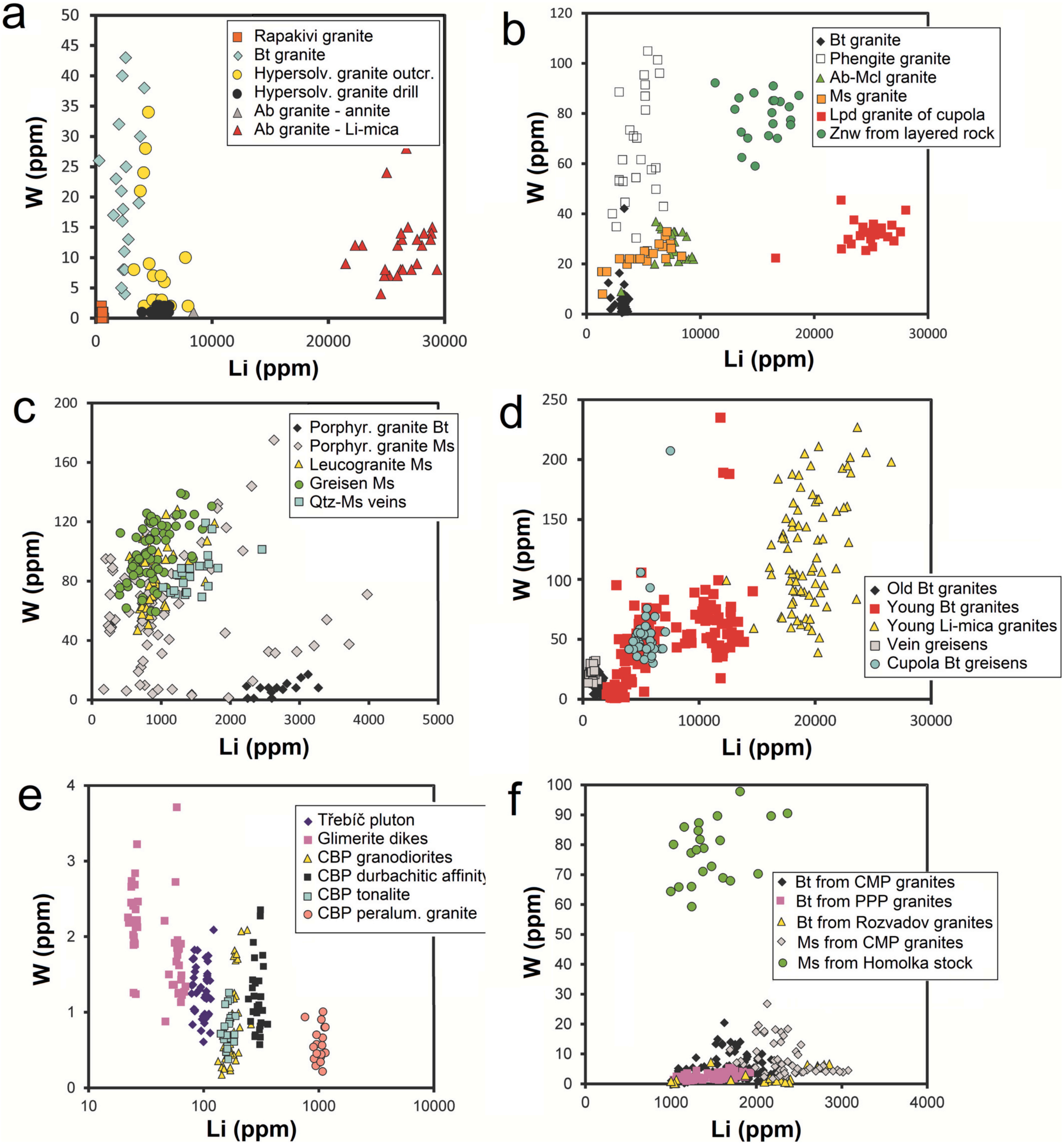

Fig. 5. Variation in W-contents in micas from selected granite plutons: a, Madeira; b, Orlovka; c, Panasqueira; d, Nejdek; e, primitive granitoids; f, two-mica granites of Moldanubicum.

bearing granites, e.g., in the historical mining areas in Cornwall and the Erzgebirge, behaves differently in fluid-related processes. The Sn/W ratio in chondrite is ca. 17 (McDonough and Sun, 1995), and similar ratio was also found in micas. The contents of W relatively increase from phlogopites in the Central Bohemian pluton (0.2–2 ppm W, Sn/W = 40–100) to Li-micas from Beauvoir (100–350 ppm W, Sn/W = 0.5–1.5). During pluton differentiation, the W contents in mica may steadily increase, thereby showing positive W-Li correlation, as found in the Nejdek pluton (Fig. 5d), Kimi or Panasqueira (Fig. 5c). Alternatively, it may remain steady as in the case of Cínovec and Beauvoir. At Madeira pluton (Fig. 5a) and Orlovka (Fig. 5b), micas from individual rock types differ, showing no consistent trend in W contents. In muscovite–biotite systems, muscovite displays higher W contents than associated biotite (Figs. 5c, f); in annite–lepidolite assemblage at Madeira albite granite, lepidolite is clearly W-enriched (Fig. 5a).

Niobium usually reaches the highest values in mica among all HFSE: from 20 to 140 ppm Nb in primitive granitoids to 1800–2400 ppm Nb in annite from the albite granite at Madeira. The behavior of Nb during pluton evolution was found to be different. At Madeira (Fig. 6a) and Argemela, Nb contents in micas increase during pluton evolution, showing a positive Nb-Li correlation. In contrast, decreasing contents, hence a negative Nb-Li correlation, is typical for granites from the Erzgebirge (Figs. 6b, e) and Beauvoir (Fig. 6d). The greisen-stage micas are relatively poor in Nb (vein greisen in the Nejdek pluton, Fig. 6e) or have similar Nb contents as the surrounding granites, as in the case of cupola greisens at Cínovec (Fig. 6b) and Panasqueira.

The contents of tantalum increase from 1 to 5 ppm Ta in phlogopite from ultramafic rocks (Fig. 7f) to 150–200 ppm Ta in zinnwaldite from

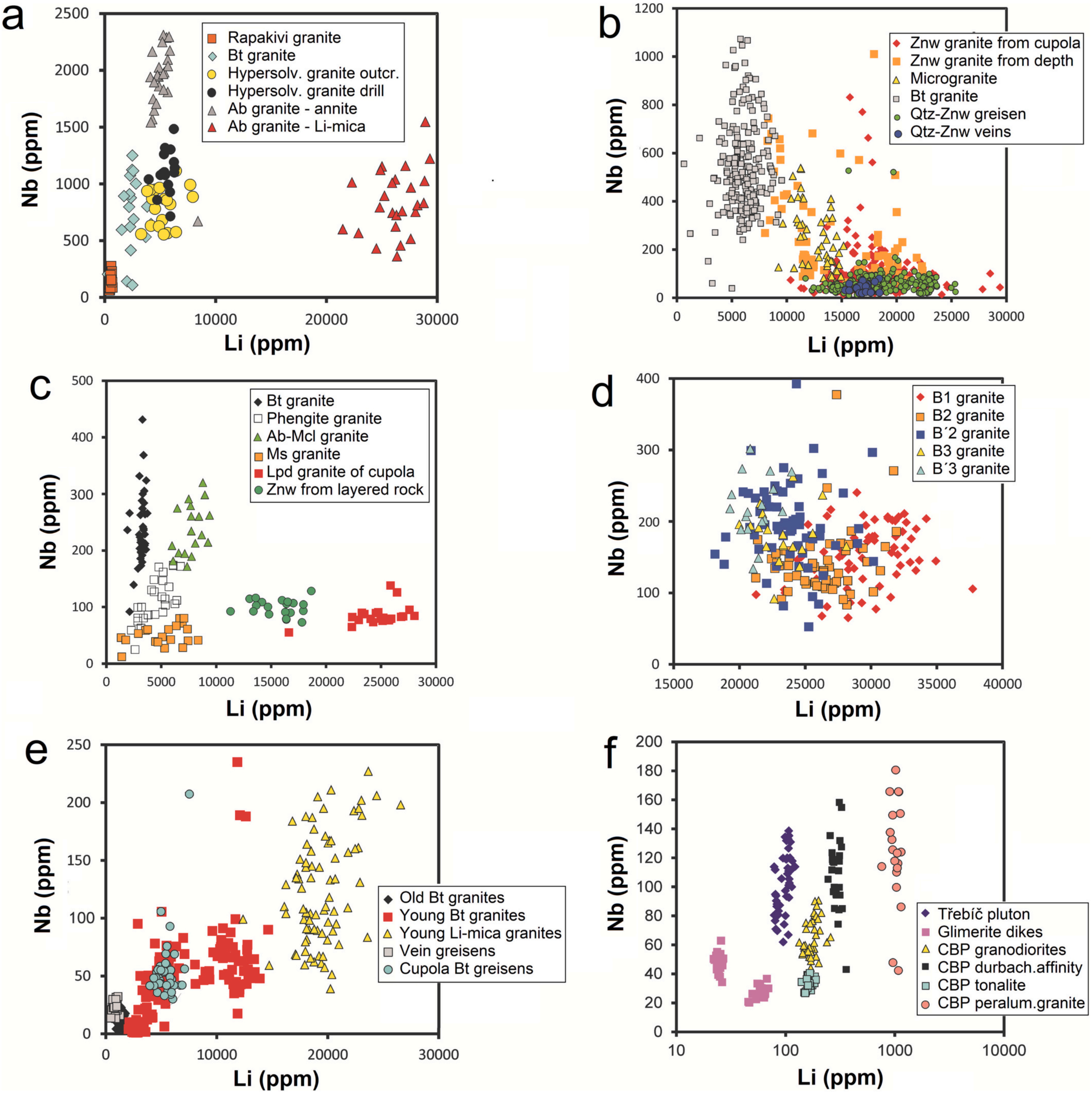

Fig. 6. Variation in Nb-contents in micas from selected granite plutons: a, Madeira; b, Cínovec; c, Orlovka; d, Beauvoir; e, Nejdek; f, primitive granitoids.

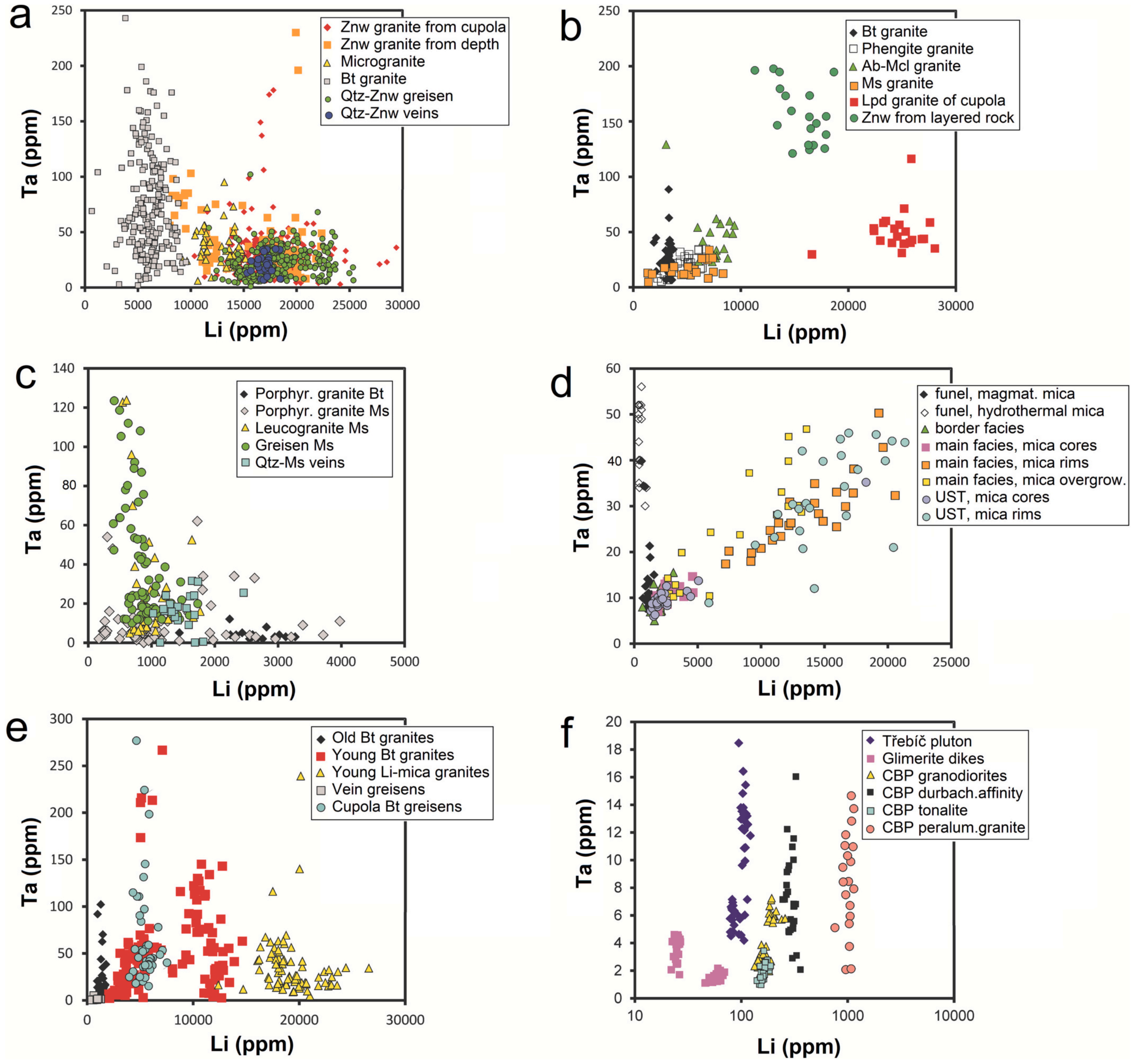

Fig. 7. Variation in Ta-contents in micas from selected granite plutons: a, Cínovec; b, Orlovka; c, Panasqueira; d, Argemela; e, Nejdek; f, primitive granitoids.

banded aplo-pegmatites from Orlovka (Fig. 7b) and 100–600 ppm Ta in siderophyllite from the Kimi stock. Generally, the dispersion of Ta values in individual rock types is wide, particularly in biotites from relatively less evolved pluton facies such as Cínovec and Nejdek (Figs. 7a, e), which makes any genetic interpretations rather difficult. Nevertheless, a general Ta decrease during pluton fractionation was found in the Madeira, Cínovec and Nejdek plutons, while an increase in Ta is obvious at Argemela (Fig. 7d). The behavior of Ta during greisenization is similar to that of Nb: relatively high contents (up to 120 ppm Ta, Fig. 7c) were found in greisen muscovite in Panasqueira, while <50 ppm Ta were found in zinnwaldite from greisen at Cínovec (Fig. 7a). Note that the Cínovec mica is associated with columbite, while no Ta minerals were found in Panasqueira greisen.

The Nb/Ta ratio, amounting at 17 in chondrites (McDonough and Sun, 1995), is highly variable in the studied micas. While values similar to those in chondrites, i.e., 15–20, were found in early magmatic micas from Panasqueira, Argemela (Fig. 8c) and primitive granitoids of the Bohemian Massif, the ratio increases to 50 in micas from peralkaline albite granite from Madeira (Fig. 8a). In contrast, relative Ta enrichment was found in Li-micas from the strongly peraluminous Nejdek pluton (Nb/Ta of ca. 5) and from Beauvoir (Nb/Ta = 2–5, Fig. 8d), and up to 0.5 in zinnwaldite from Orlovka (Fig. 8b). When compared with the bulk-rock Nb/Ta values, annite and lepidolite from the Madeira albite granite (Nb/Ta ~ 60) is Ta-impoverished by a factor of about 10 (bulk value Nb/Ta ~ 5–10, Costi et al., 2009), which is in agreement with the theoretical expectation (Stepanov and Hermann, 2013). A different picture is seen in the case of Orlovka: the bulk-rock Nb/Ta value evolved from ca. 2 in the deeper part of the pluton to ca. 0.5 in the cupola, and finally to 1 in the late banded aplo-pegmatite bodies (Badanina et al., 2004). In the same succession, this value in mica evolved from ca. 6 to 2 and finally to 0.5; micas from the late rocks are relatively Ta-enriched compared to the bulk values.

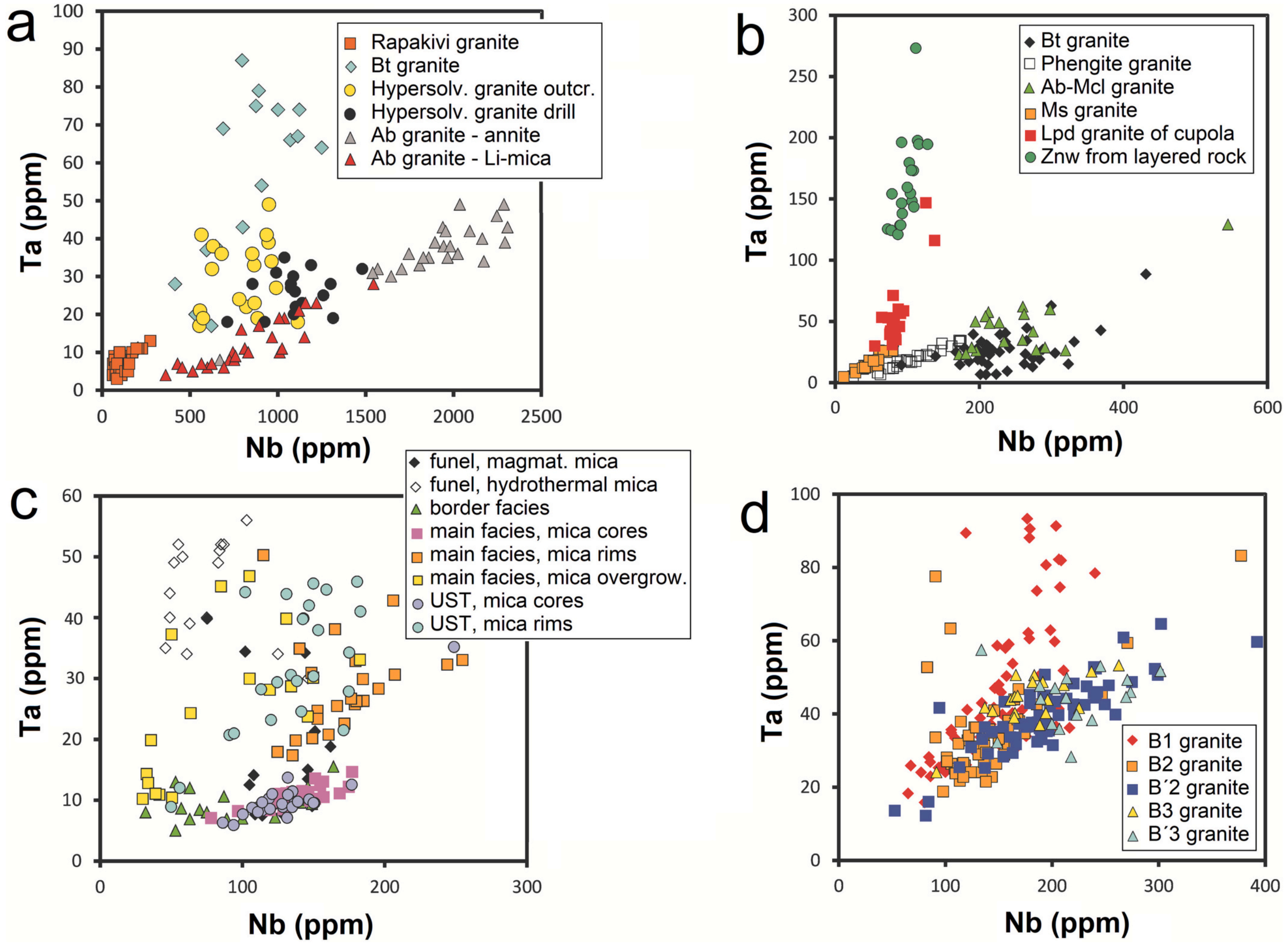

Fig. 8. Variation in Nb/Ta value in micas from selected granite plutons: a, Madeira; b, Orlovka; c, Argemela; d, Beauvoir.

5.3. *Rare alkalis Rb and Cs*

Elements Rb and Cs are typical LILE (large-ion lithophile elements), geochemically similar to potassium, Rb being about one order of magnitude more abundant than Cs in granitic environment. Minerals with dominant Rb or Cs contents are very rare and their occurrence is restricted to extremely fractionated LCT (i.e., Li, Cs, Ta-bearing) pegmatites (Černý et al., 1985). Therefore, Rb and Cs usually enter crystal lattices of common K-bearing silicates, particularly K-feldspar (Rb) and micas (Rb and Cs). While mica is the only common Cs host in granites, Rb is distributed between mica and K-feldspar, and the Cs/Rb values in mica may be thus significantly higher than those in bulk-rock analyses. The enrichment in Rb and Cs in some micas from pegmatites can achieve levels high enough to consider them as Rb- and Cs-mica endmembers (Rb- and Cs-dominant analogous of polylithionite), although such mica poles have not been named yet (Černý et al., 2003; Wang et al., 2004). The highest Rb and Cs contents reported from granites are much lower: 5.18 wt% Rb_2O (0.29 apfu Rb) and 0.95 wt% Cs_2O (0.05 apfu Cs) in lepidolite from Yashan granites, China (Li et al., 2015).

The contents of Rb in the studied micas increase from about one-hundred ppm in biotites from tonalites and granodiorites of the Central Bohemian pluton to several thousand ppm in W- and Sn-bearing plutons (Panasqueira, Argemela, Nejdek) and up to 30–45 thousand ppm (i.e., >4 wt% Rb_2O) in albite-cryolite granite from Madeira, which equals the contents found in associated annite and lepidolite (Fig. 9a). During the evolution of particular plutons, the contents of Rb in mica often show a positive correlation with Li contents, reflecting the general fractionation trend of parental melt. Such more-or-less regular evolution was found, for example, in the Kimi stock, Cínovec pluton (Fig. 9b), Orlovka pluton (Fig. 9c), Argemela or Nejdek pluton. In other plutons, like the Panasqueira or Beauvoir (Fig. 9d), the correlation between Rb and Li is only poor. In less fractionated two-mica granites from the Moldanubicum, the contents of Rb are slightly higher in biotites (usually <1000 ppm) than in associated muscovite (<500 ppm).

Cs is not as common as Rb (chondritic value Cs:Rb = 1:12, McDonough and Sun, 1995). The highest contents of Cs were found in micas from strongly peraluminous granites like Beauvoir (500–4500 ppm, Fig. 10d) and Nejdek (<100–2500 ppm, Fig. 10e), while micas from the majority of peraluminous granites (i.e., Panasqueira and Argemela, Fig. 10c) mostly contain <200–300 ppm Cs. Micas from peralkaline granites (Madeira pluton, Fig. 10a) and metaluminous granites like Cínovec (Fig. 10b), Orlovka and Kimi contain several hundred ppm Cs, with the maximum of 1200 ppm Cs at Cínovec.

Compared to Rb and Li, the dispersion of Cs values in individual rock types and even samples is much higher, resulting in only a weak (e.g., Argemela, Fig. 10c) or no Cs-Li correlation (e.g., Nejdek, Fig. 10e).

The Cs/Rb ratios in the studied micas are generally lower than that in the chondrites in the case of peralkaline, subaluminous and some peraluminous granites (1:20 to 1:30 at Madeira, 1:50 in Li-micas from Orlovka, 1:30 in the early micas from Argemela), but increase in some strongly peraluminous granites (max. 1:4 at Beauvoir and 1:3 at Nejdek). The correlation between Cs and Rb is only weak in micas from Madeira, Panasqueira and Argemela, while no correlation was found in the most Cs-enriched micas from Beauvoir, Nejdek and Cínovec.

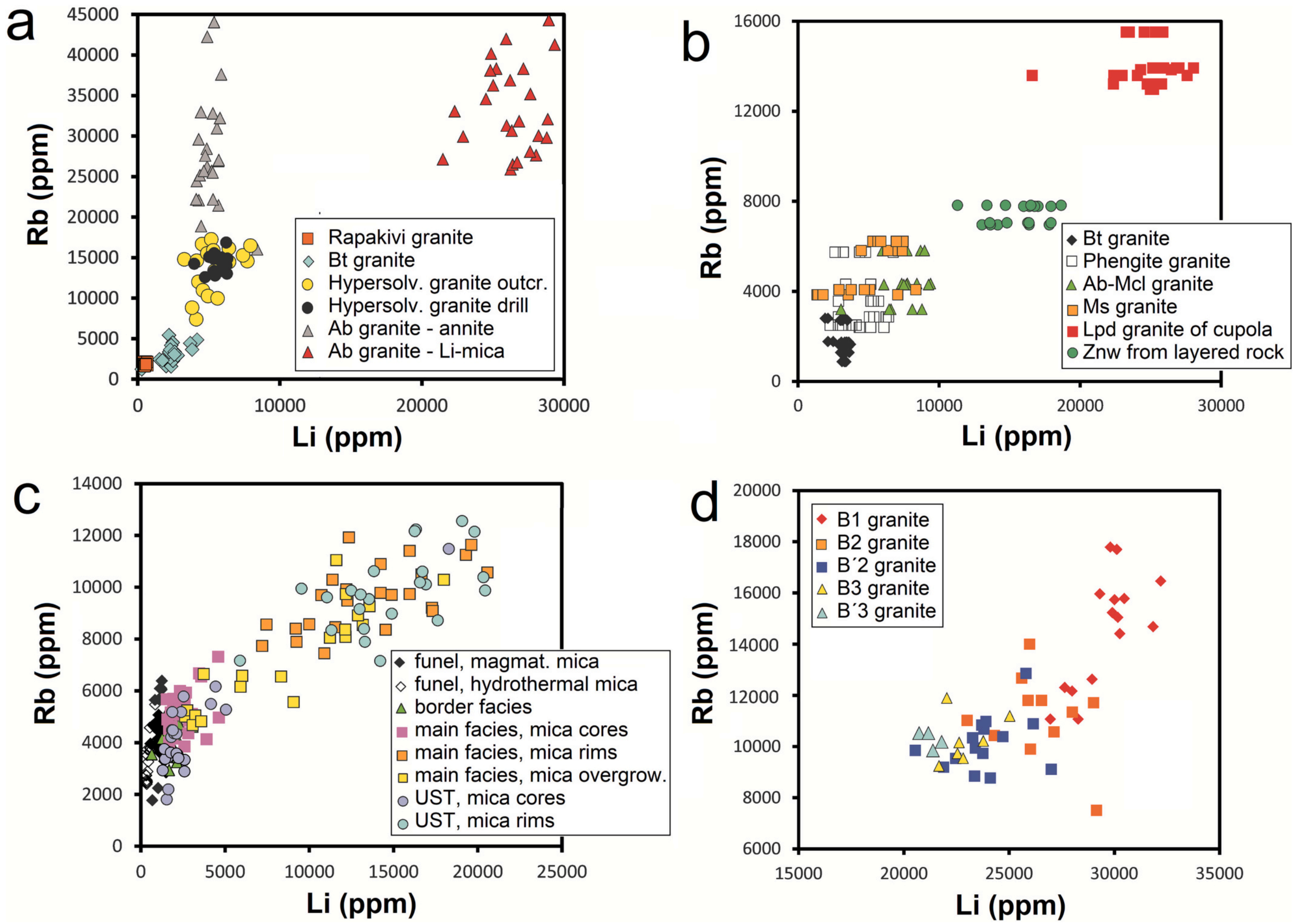

Fig. 9. Variation in Rb-contents in micas from selected granite plutons: a, Madeira; b, Orlovka; c, Argemela; d, Beauvoir.

At Argemela, a strong coupled Li, Rb and Cs enrichment (Figs. 9c, 10c) distinguishes the late magmatic lepidolite rims of mica crystals from their early magmatic muscovite cores (compare Figs. 3b, c).

5.4. *Scandium*

Sc is geochemically rather similar to Fe and its behavior in granites is still poorly understood. The contents of Sc in the studied micas were found to range from 100 to 200 ppm in some biotites from Cínovec (Fig. 11b) and Panasqueira and in zinnwaldite from Kimi, to <1 ppm in lepidolites from Argemela (Fig. 11d) and Beauvoir. Maximum Sc contents, up to 300 ppm, were found in phengite from Orlovka (Fig. 11c). Micas from primitive granitoids contain 10–60 ppm Sc (Fig. 11f). During fractionation, along with a decrease in Fe contents, Sc also decreases at Nejdek (Fig. 11e), Madeira (Fig. 11a) and Argemela (Fig. 11d), but remains generally stable in the case of Cínovec (Fig. 11b). During greisenization, Sc contents remain unchanged in zinnwaldite at Cínovec (Fig. 11b) but Sc completely disappears in muscovites from the Nejdek vein greisens (Fig. 11e) and from the Panasqueira greisen cupola and quartz lodes.

6. Vertical zoning of RMG plutons expressed in mica chemistry

In three of the studied rare-metal granite plutons, deep boreholes were realized to investigate vertical zoning of the plutons and roots of mineralizing systems. Changes in the macro- and microchemical composition of micas and the role of micas in late magmatic/hydrothermal processes leading to the origin of ore deposits are the main herein commented issues that have been extracted from the huge amount of data yielded by the boreholes.

6.1. *Cínovec (Erzgebirge, Czech Republic)*

The Cínovec very deep borehole CS-1 is the oldest (realized in 1960–1963) and also the deepest (1596 m) borehole as yet realized in rare-metal granites. Different models of mineralization were published recently by Johan et al. (2012) and Breiter et al. (2017b); micas were studied by Breiter et al. (2019a).

Vertical changes in mica chemistry are illustrated in Fig. 12. The distribution of major mica constituents like Li, Rb and F (Fig. 12a) reveals the general structure of the pluton, with zinnwaldite granite from the top of the intrusion to a depth of 735 m, and biotite granite following to greater depths. The distribution of major elements is relatively homogeneous among micas from these two basic units. It should be also noted that the composition of mica from greisen bodies within the cupola is nearly identical to that from the surrounding zinnwaldite granite, in both major and trace elements! However, the contents of HFSE (Fig. 12b, c) are more varied and irregular. The contents of Sn and Nb in mica, although having different general geochemical properties, behave similarly: they show a marked decrease upwards. In biotite granites, biotite is the major host of Sn and Nb (mostly 200–600 ppm Sn, 400–700 ppm Nb), while accessory magmatic cassiterite and columbite crystallized early in the zinnwaldite granite. As a result, zinnwaldite is relatively Sn, Nb-poor (mostly <200 ppm Sn and Nb). The distribution of Ta is much more regular than that of Nb with only a mild decrease upwards, which implies an upwards decrease in the Nb/Ta value, as the

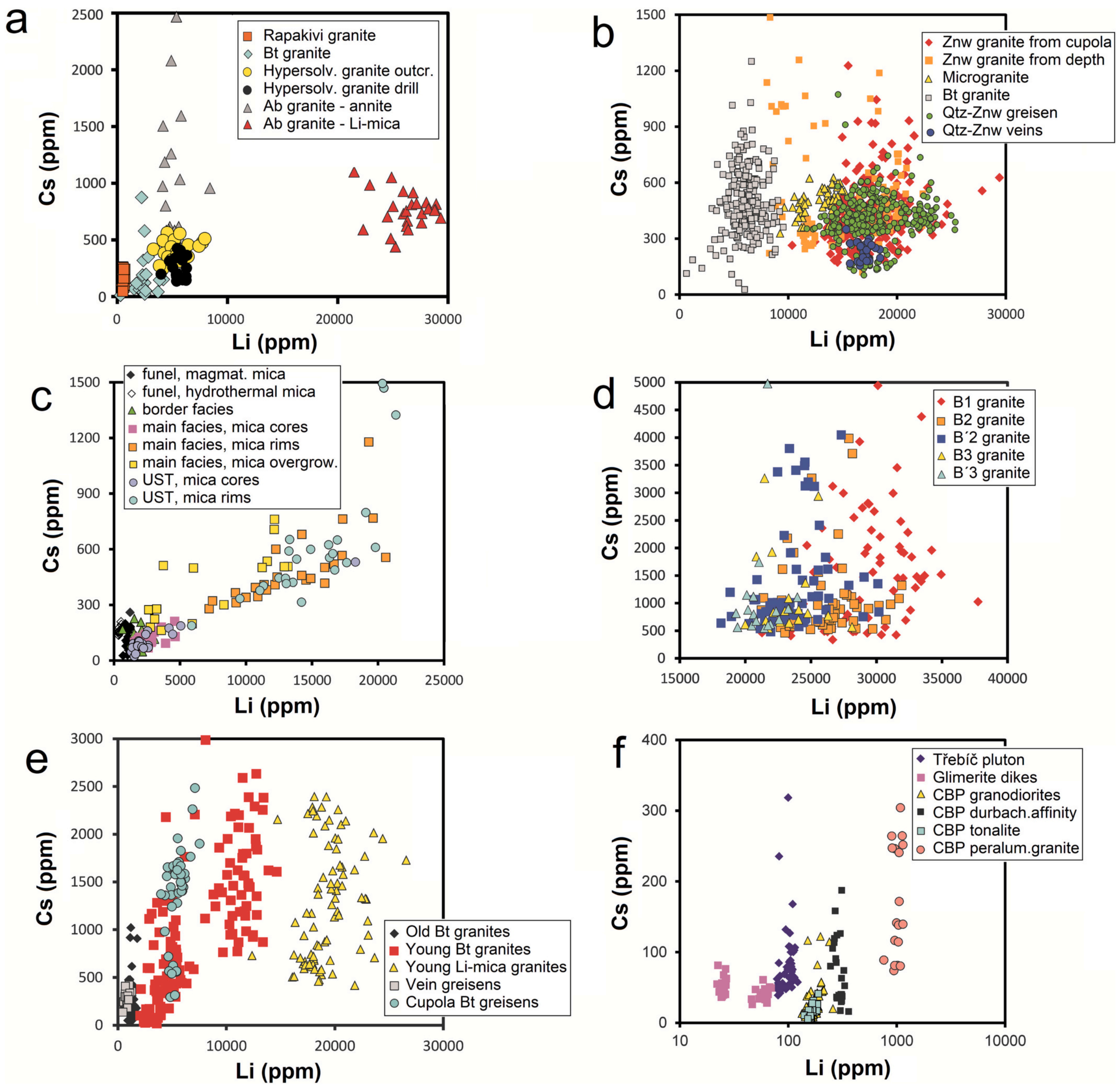

Fig. 10. Variation in Cs-contents in micas from selected granite plutons: a, Madeira; b, Cínovec; c, Argemela; d, Beauvoir; e, Nejdek; f, primitive granitoids.

geochemical theory requires anyway (Stepanov and Hermann, 2013). However, the Nb/Ta value itself strongly fluctuates, probably reflecting changes in associated oxide minerals assemblage (rutile, columbite, ixiolite; Breiter et al., 2017b). The contents of W in mica are relatively low and stable through the whole analyzed profile.

6.2. Beauvoir (France)

The Beauvoir igneous system studied by a 900 m deep borehole GPF-1 comprises two successively emplaced comagmatic portions of granite melt, units B and B´, which fractionated independently (Raimbault et al., 1995). Bulk-rock composition indicates a strong upwards directed enrichment in volatile and trace elements in both units (Cuney et al., 1992; Raimbault et al., 1995). The Beauvoir melt was strongly geochemically evolved already at the start of intrusion, thus the contrast between the less evolved and the most evolved parts of the system is not as sheer as in the case of the Cínovec deposit. Within borehole profile, mica composition shifts from zinnwaldite in unit B´3 to nearly ideal lepidolite in the uppermost unit B1, as already shown by Monier et al. (1987). The first reliable trace-element data of micas were published recently by Monnier et al. (2022). Our data (10 samples) show an upward increase of Li, Rb and F (4.6 → 6.6 wt% Li_2O, 1.1 → 1.8 wt% Rb_2O, 7.2 → 8.5 wt% F, Fig. 12d). At the same time, Fe disappears (7.5 → 0.3 wt% FeO). The distribution of Sn, W, Nb and Ta is irregular and without any clear trend (Fig. 12e, f), not following the bulk-rock trends to strong upwards enrichment (Raimbault et al., 1995). In analogy with Cínovec, it can be speculated that relatively early crystallization of columbite and cassiterite in the upper part of the system decreased the contents of these elements in the melt already prior to mica crystallization. Data by Monnier et al. (2022), for comparison also presented in Fig. 12, show

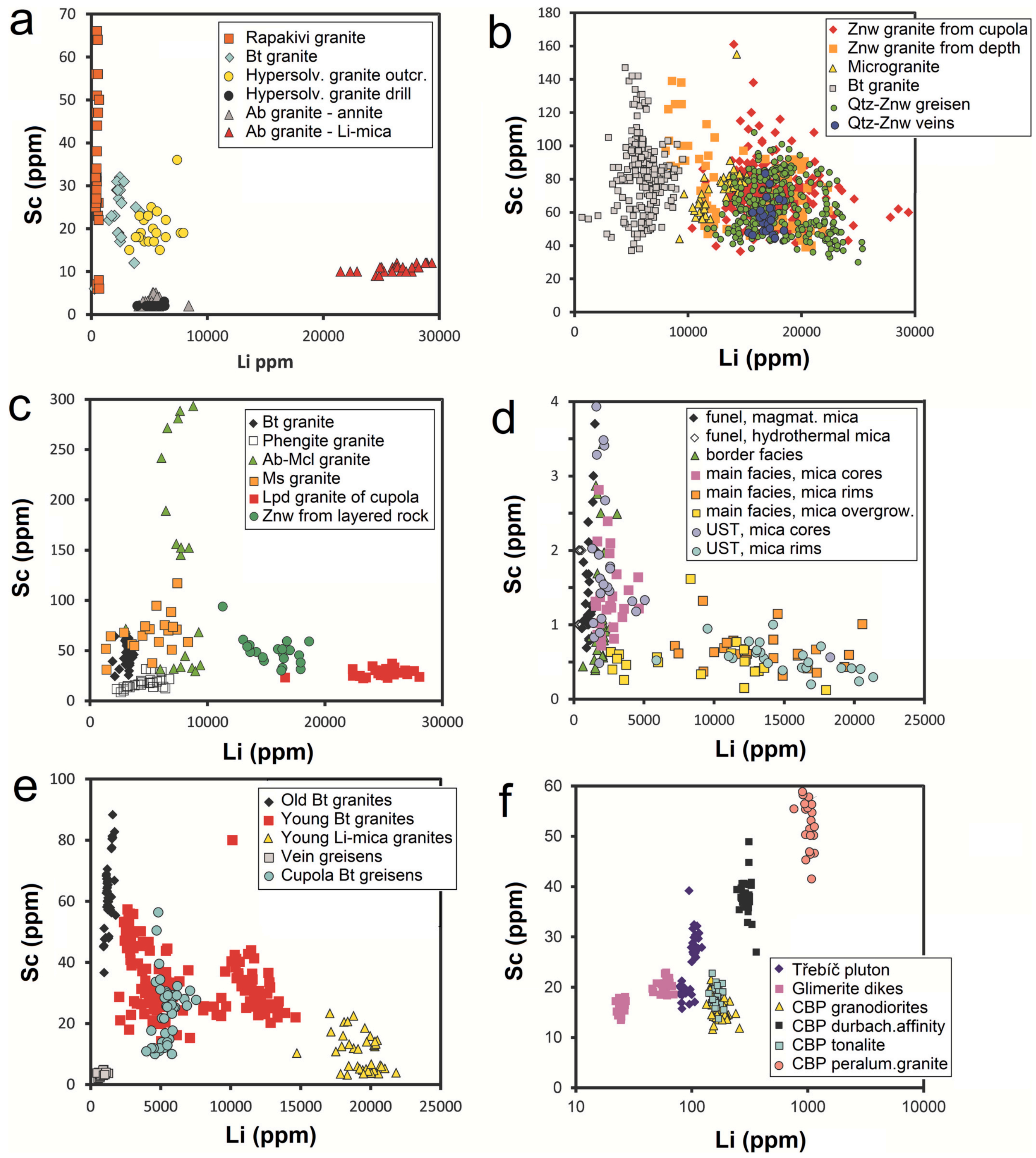

Fig. 11. Variation in Sc-contents in micas from selected granite plutons: a, Madeira; b, Cínovec; c, Orlovka; d, Argemela; e, Nejdek; f, primitive granitoids.

generally similar trends although some discrepancies, namely at distribution of W and Nb, point to local inhomogeneity. Even more samples would be needed to capture the vertical evolution in its full complexity.

6.3. Orlovka (eastern Siberia, Russia)

The exploration of the Orlovka deposit involved drilling of several boreholes 300–400 m long (Badanina et al., 2004). Nevertheless, due to the lack of preserved cores, only a simplified idealized vertical evolution of mica can be outlined. Among the presented vertical sections, the Orlovka micas are the most diversified, comprising not only members of the biotite–zinnwaldite–lepidolite series, but also micas of muscovite–-phengite composition (Fig. 2d). Nevertheless, the Li contents increase steadily upwards from 1 to 5.5 wt% Li_2O. Similarly, F contents increase from ca. 2 to 8 wt%, while Rb contents are irregular and relatively low (Fig. 13a). The contents of rare metals Sn and Nb generally decrease

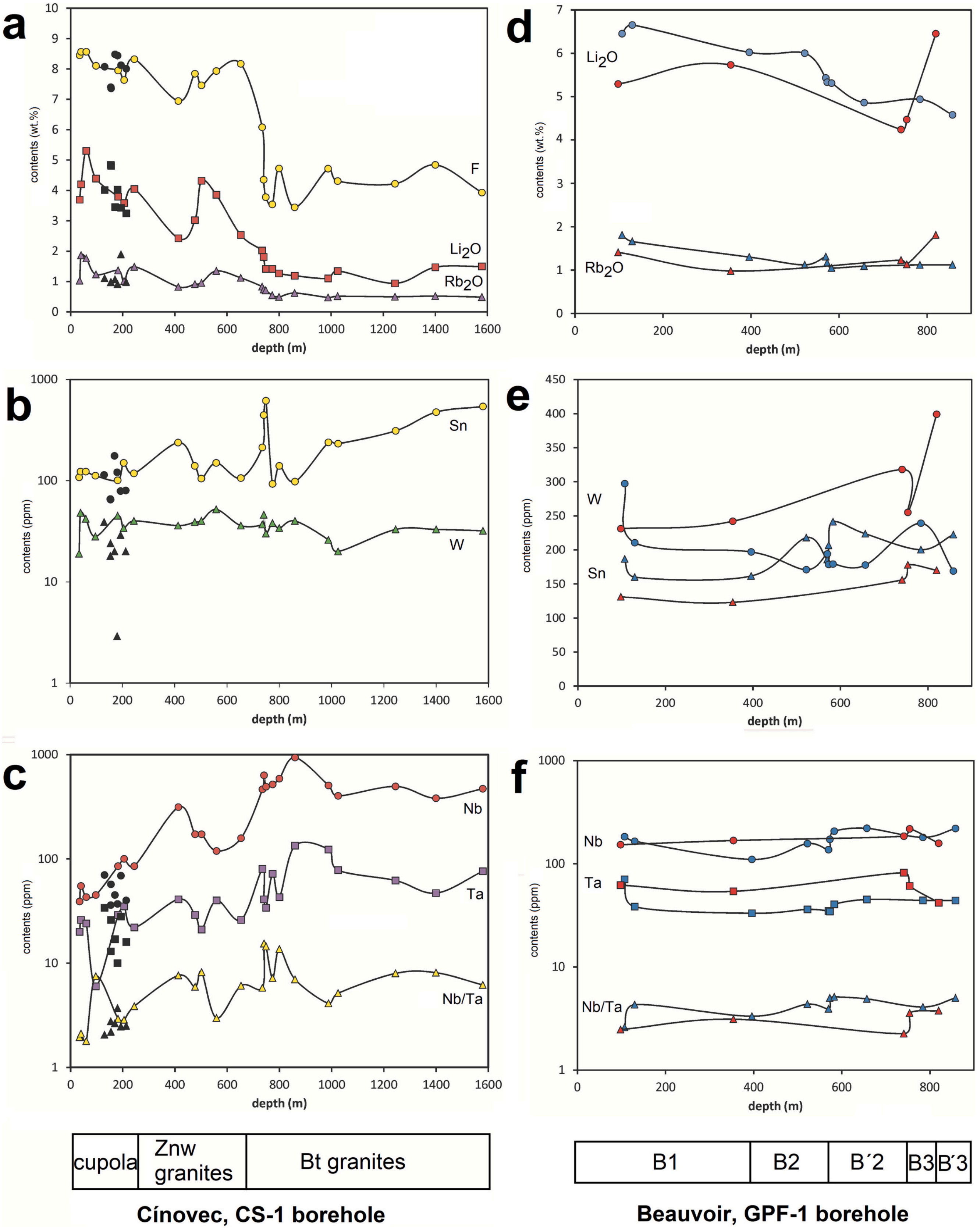

Fig. 12. Comparison of vertical evolution of mica composition in granites and greisens in the Cínovec pluton (left column, a–c) with composition of mica from granites in the Beauvoir granite stock (right column, d–f). At Cínovec: colour symbols- granites, black symbols-greisens. At Beauvoir: blue symbols- author's data, red symbols- data from Monnier et al. (2022). (For interpretation of the references to colour in this figure legend, the reader is referred to the web version of this article.)

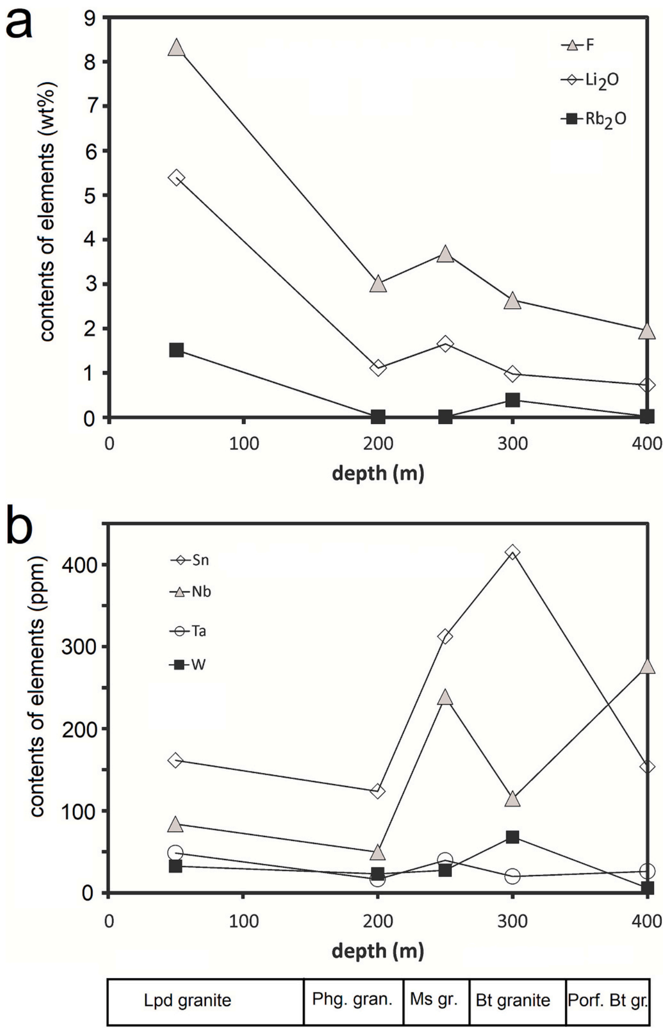

Fig. 13. Vertical evolution of mica composition in the Orlovka pluton: a, F, Li_2O, Rb_2O; b, Sn, W, Nb, Ta.

from biotite upwards to lepidolite, while the contents of W and Ta are relatively low, mostly <50 ppm, and without any clear trend (Fig. 13b). Somewhat surprising are the relatively low contents of Li and F together with the very high W and Ta contents in zinnwaldite (Table 6) from the latest rock within the system, i.e., the aplo-pegmatite layers crosscutting the lepidolite granite of the cupola (not included in Fig. 13).

7. Mica in greisens and quartz lodes

Greisen-type Sn-W deposits are typical for shallow-level intrusions of rare-metal granites. This type of mineralization is widespread particularly in European Variscan terranes, where examples in the Erzgebirge were studied in detail (Breiter et al., 1999, 2017b; Johan et al., 2012). Mica is, besides quartz, the most common constituent of the greisens, locally accompanied by rather low amounts of topaz, tourmaline, K-feldspar or apatite. Data discussed here comprise greisen samples from Li-rich Sn-W (+Rb, Nb, Ta, Sc) deposit of Cínovec, the Li-rich magmatic/hydrothermal system at Beauvoir (Monnier et al., 2022), Li-poor cupola- and vein-type greisen bodies in the western Erzgebirge (Nejdek pluton) and from the Li-poor W deposit of Panasqueira, Portugal. Greisen at Cínovec contains zinnwaldite while micas from other greisens are classified as muscovite (Beauvoir), muscovite-phengite (Panasqueira quartz lodes and Nejdek vein greisens) or biotite (Nejdek cupola-type greisens). Greisen micas are closely related to the “ore minerals” cassiterite and wolframite in space, and also often in time, i.e., they seem to be products of crystallization of the same fluid (Štemprok, 1987). Nevertheless, the contents of Sn, W and other “ore” elements in micas are highly variable and do not correlate with the contents of associated ore minerals: Panasqueira quartz lodes, richly mineralized with wolframite, contain muscovite with similar W contents as the ore-free greisen cupola.

The highest Sn contents among greisen-related micas were found in muscovite from not-mineralized greisen inside the Beauvoir granite (ca. 800–1500 ppm Sn, Fig. 14a). The highest W contents, 80–140 ppm W, were found in mica-poor portions of the greisen body in the Panasqueira cupola, although Sn and W mineralization in the Panasqueira greisen is poor and sub-economic (Marignac et al., 2020). In contrast, the cupola greisen at Cínovec, having been long mined for cassiterite and wolframite, contains zinnwaldite poor in both Sn and W (<200 and <40 ppm, respectively). Moreover, the Sn/W value in greisen mica varied strongly: from >100 in muscovite from Beauvoir to 2–3 in zinnwaldite from Cínovec or muscovite from Panasqueira. As for Nb and Ta (Fig. 14b), the highest Nb contents, up to 500 ppm, were found in muscovite from the Nejdek vein greisens (Nb/Ta ~ 5), which are free of Nb, Ta minerals. On the other hand, zinnwaldite from Cínovec, associated with small amounts of columbite, is poor in both Nb and Ta (<100 ppm Nb, <50 ppm Ta). The only mica with Ta > Nb was found in the Beauvoir greisen: 20–38 ppm Ta vs. <10 ppm Nb (Monnier et al., 2022).

Micas from lodes (mineralized quartz veins) generally contain lesser

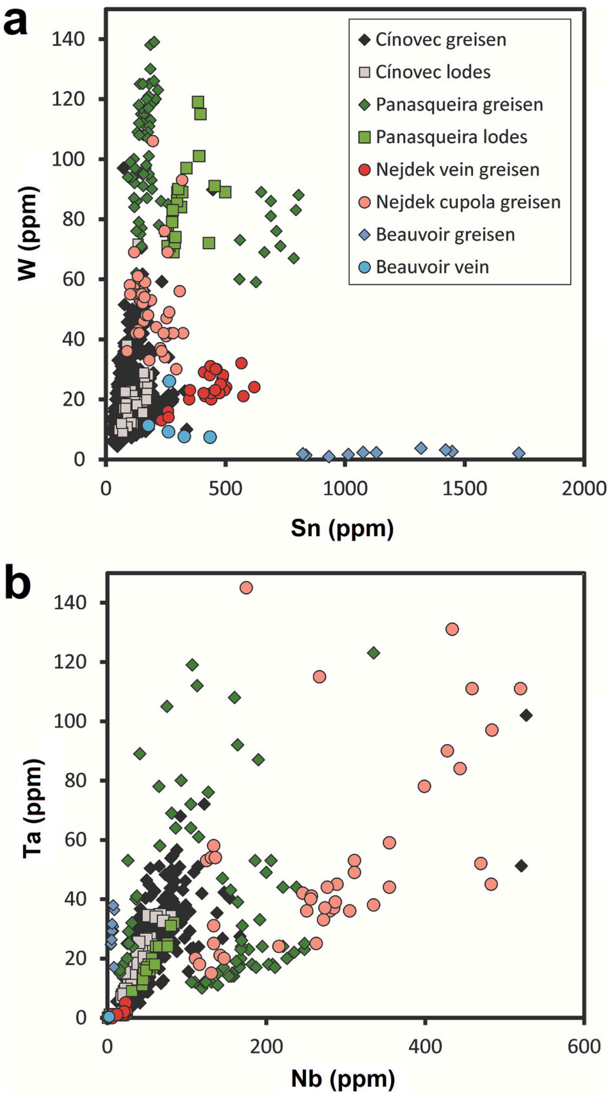

Fig. 14. Contents of trace elements in micas from greisen and quartz lodes: a, Sn vs. W; b, Nb vs. Ta. Data from Beauvoir according to Monnier et al. (2022).

amounts of rare metals than micas from associated greisen; an exception is W-rich muscovite from Panasqueira.

Taken together, micas immediately associated with ore minerals contain lower amounts of particular ore elements than micas in non-mineralized or only poorly mineralized greisen bodies.

8. Two-mica assemblage in rare-metal granites

The assemblage of two distinct magmatic mica types being at chemical equilibrium is usually restricted to less evolved peraluminous muscovite-biotite granites, usually termed as “two-mica granites”. Examples of these granites from the South Bohemian batholith are shown in this review: muscovite from a typical two-mica Eisgarn granite is, compared to associated biotite, richer in all monitored rare alkalis (0.46 vs. 0.36 wt% Li_2O, 1615 vs. 1370 ppm Rb and 208 vs. 156 ppm Cs) and rare metals (150 vs. 80 ppm Sn, 31 vs. 4.5 ppm W, 246 vs. 190 ppm Nb and 20 vs. 14 ppm Ta).

Only a single species of mica usually crystallized in volatile-rich rare-metal granites. When two different compositions of mica grains/zones/patches are still found, this is probably a result of (i) successive crystallization at changeable conditions, i.e., magmatic zoning such as that at Argemela, or (ii) hydrothermal alteration/re-equilibration such as that, for example, producing siderophyllite vs. phengite at Kimi.

The association of two different micas with textural signs of magmatic origin and long-term physico-chemical equilibrium was, among all the studied RMG plutons, found only in the Madeira albite granite, as already referred by Costi et al. (2009). Here, Zn, Rb-rich annite forms intimate intergrowths with Rb, Zn-rich lepidolite. In detail, the two-mica assemblage is complicated by intergrowths with riebeckite, cryolite, magnetite, feldspars, etc. (Fig. 3e, f). The lepidolite/annite ratio increases in cryolite-rich parts of albite granite crystallizing from particularly F-rich portion of the residual melt. The two mica species have a sharp boundary with no reaction zone (Fig. 3a) although differ significantly: 53–55 vs. 40 wt% SiO_2, 13–14 vs. 7 wt% Al_2O_3, 6–8 vs. 24–26 wt% FeO, and 8.5 vs. 4 wt% F, respectively. We were not able to analyze trace elements in annite from the intergrowths due to the small size of the grains and the number of inclusions. Still, we can compare lepidolite from the intergrowths with annite from another sample forming individual grains. In such comparison, lepidolite is relatively enriched in Li (5.5 vs. 1 wt% Li_2O) and rather surprisingly in W and Sc, while annite is enriched in Sn, Nb, Ta, Tl, and Ga. The content of Cs is almost the same.

Another example to be mentioned is the Colette granite, France, in a close proximity of Beauvoir. The Colette granite contains zinnwaldite and muscovite, the former being richer in Li (6200 vs. 2400 ppm), Rb (2500 vs. 1550 ppm), Cs (1400 vs. 100 ppm), Nb (419 vs. 234 ppm) and Ta (82 vs. 36 ppm), but poorer in Sn (193 vs. 319 ppm) and W (48 vs. 159 ppm) (Monnier et al., 2022). Thus, the greater ability of muscovite, compared to other mica species, to absorb particularly Sn and W is generally valid.

9. Discussion

9.1. What are the maximum contents of minor and trace elements in micas?

There still exists a surprisingly low amount of reliable data about the contents of minor and trace elements in granitic micas. A somewhat better situation is observed in pegmatites, especially thanks to the activity of P. Černý and his coworkers (review in Černý et al., 1985). Moreover, all analyses of trace elements acquired prior to about the year 2000 were performed using classical chemical methods from mono-mineral mica concentrates. Particularly the contents of HFSE were exaggerated due to micro-inclusions of accessory minerals like rutile, cassiterite and columbite. Only the laser-ablation ICP-MS data published during the last two decades provide a realistic picture of HFSE contents. Of course, the contents of Rb, Cs and Zn may be high enough to be analyzed by a microprobe.

As mentioned above, the contents of Rb and Cs may exceed the contents of K, forming new mica endmembers, not approved by IMA yet. Wang et al. (2004) reported max. 0.79 apfu Cs in lepidolite from the Yichun granite, China. Černý et al. (2003) reported phlogopite with 0.92 apfu Cs and polylithionite with 0.82 apfu Rb from the Red Cross Lake pegmatite, Canada.

The Zn-dominant mica hendricksite, a Zn-analogue of annite, was firstly described from Zn-rich metamorphic assemblage at Franklin, New Jersey, USA (no analysis published!), by Frondel and Baum (1974). Zn-enriched micas reported from other localities are not Zn-dominant.

The highest published Sn content in mica from greisenized domain within Beauvoir granite reaches 800–1500 ppm (Monnier et al., 2022) which is roughly similar to values found at Madeira (up to 1300 ppm Sn, Fig. 4a) and higher than zinnwaldite from the Cínovec Sn-W deposit (up to 800 ppm). The highest published W content of 296 ppm in lepidolite from Beauvoir (Monnier et al., 2022) is well comparable with our values from this granite (100–350 ppm W) and higher than values from Nejdek zinnwaldite (scarcely >200 ppm) and all other studied localities (usually <140 ppm W, Fig. 5).

The published contents of Nb are mostly <100 ppm (Legros et al., 2018; Li et al., 2015; Van Lichtervelde et al., 2008; Xie et al., 2015), the only exception is zinnwaldite from the Colette granite with about 400 ppm Nb (Monnier et al., 2022). This is substantially less than found in some of plutons studied in this paper: 500–1000 ppm Nb in Kimi and Cínovec, and 500–2300 ppm Nb in Madeira (Fig. 6). In the case of Ta, published values in the range of 100–200 ppm (Li et al., 2015; Roda-Robles et al., 2012; Van Lichtervelde et al., 2008) are similar to those found in Cínovec, Nejdek, Orlovka or Panasqueira (Fig. 7) while 100–600 ppm Ta was found in Li-annite from the Kimi stock.

The highest Sc content in mica so far was reported from Li-rich micas from the Tanco pegmatite in the range of 16–180 ppm (Van Lichtervelde et al., 2008), which is roughly comparable with the values found at Cínovec and Orlovka (Fig. 11).

9.2. Evolution of mica chemistry via fractional crystallization

According to general geochemical rules (Goldschmidt, 1937), concentrations of some trace elements are expected to increase during fractionation of granitic melts. In addition, concentrations of these elements in some rock-forming minerals, including micas, are also expected to increase. Partition coefficients between silicate melt and Fe-bearing mica for F, Rb, Cs were studied by Icenhower and London (1995), those for Li, Rb, Cs and some of HFSE were studied by Bea et al. (1994), and those for Nb and Ta by Stepanov and Hermann (2013). The published values differ significantly, although all authors came to the conclusion that $D^{Bt/melt}$ is >1 for Li, Rb and Nb, but <1 for Cs. The values for Ta vary around 1. The coefficients for Sn and W were never experimentally studied but are expected to be substantially higher than 1 comparing the Sn contents in micas and in their parental granites. Modal contents of mica in most granites vary around 5%. Therefore, at $D^{mica/melt}$ lying in range of 1–10, the contents of Sn and W in the residual melt increase, if not consumed by accessory minerals.

Acording to a large number of published analyses (Bailey, 1984; Černý and Burt, 1984; Tischendorf et al., 2001), the contents of Li and Rb in micas steadily increase during magma fractionation following theoretical expectations (Goldschmidt, 1937). Li in granitic melt enters mainly the crystal lattice of micas, ranging from several ppm to 5–6 wt% Li_2O in late lepidolite, while its share in other silicates is negligible. Thus, the incorporation of Li in mica is really controlled by the Li contents in the melt and its partition coefficient. For Rb, this process is complicated by its parallel incorporation in K-feldspar. The Rb partition coefficient mica/Kfs was found to vary around 2 (Icenhower and London, 1995, 1996) but the Rb distribution between mica and Kfs in a specific rock can be influenced by timing of mica vs. feldspar crystallization and/or postmagmatic re-equilibration.

The contents of HFSE in mica, in our case Sn, W, Nb and Ta, are influenced by early crystallization of rutile, which may absorb large amounts of all these elements. In the case of high contents of Sn and Nb in the melt, the process is also affected by the crystallization of disseminated magmatic cassiterite and columbite. The higher the contents of Sn, Nb and Ta in the melt, the higher the amounts of cassiterite and columbite that crystallize, and the lower the Sn and Nb contents in the subsequent crystallizing micas. Such evolution is illustrated by decreasing contents of Sn, Nb and Ta in a succession from biotites in the early pluton constituents to Li-micas in the late pluton facies, as shown for Cínovec (Breiter et al., 2017a) and some other plutons (Figs. 4, 6, 7).

The Nb/Ta values in mica (biotite) in peraluminous conditions were experimentally estimated at 2.2–3.2 (Stepanov and Hermann, 2013); such values imply that micas should be enriched in Nb relative to the parental melt, while the residual melt is enriched in Ta.

9.3. *Micas as a HFSE reservoir*

The contribution of mica to the bulk-rock budget of Rb and some HFSE was studied at Cínovec by Breiter et al. (2019a) and at Beauvoir by Monnier et al. (2022). In a succession from early biotite to late zinnwaldite granites at Cínovec, the share of mica in bulk-rock Rb increases from 20 to 80%, while the content of K-feldspar decreases and mica becomes the dominant Rb host. In contrast, the share of mica in bulk-rock Sn, Nb and Ta decreases (50–80 → 5–10%, 10–80 → 1–10% and 100 → <5%, respectively). Simultaneously, accessory rutile, cassiterite and columbite become common constituents of the granites.

Johan et al. (2012) hypothesized that primary micas, i.e., biotite, formed a temporary reservoir for all HFSE present in the magma. Later, during the event of Li-metasomatism, Sn, W-enriched biotite was transformed to Sn, W-poor zinnwaldite, and the liberated metals were transported to the cupola forming the actual cassiterite+wolframite greisen deposit. This model was disproved by Breiter et al. (2017b): mica in deeper parts of the pluton is very likely in the primary state, and the ore elements are supposed to have been segregated directly from the melt to hydrothermal fluids during the crystallization of a “mica-free” zone below the greisens.

A rather different role of micas during the greisenization was found at Beauvoir (Monnier et al., 2022): greisenizing fluid destroyed primary cassiterite and Sn,W-enriched lepidolite, forming extremely Sn-rich muscovite (aver. 1385 ppm Sn), while Li, Rb and W were transported away, forming, among others, exogranitic quartz–wolframite veins. In this case, the greisen has, paradoxically, lower contents of ore elements than the original granite.

9.4. *Magmatic vs. hydrothermal stage in mica evolution*

Micas from the porphyritic granite facies at Argemela represent an excellent example of a succession of early magmatic, late magmatic and hydrothermal growth, resulting in complex zoning (Breiter et al., 2022; Charoy and Noronha, 1996; Michaud and Pichavant, 2020). Subhedral–euhedral mica flakes, 0.5–2 mm in size, are composed of three distinct zones: (i) early magmatic euhedral to subhedral Li-phengitic cores, (ii) late magmatic subhedral lepidolite rims, and (iii) hydrothermal irregular overgrowths of fine-grained lepidolite or muscovite (Fig. 3b). The contents of Si, Li, Mn, Rb and F increase from cores to rims (46–47 → 48.5–50.5 wt% SiO_2; 0.5–1.0 to 2.0–4.6 wt% Li_2O; <0.2 → 0.5–0.8 wt% MnO; 0.3–0.6 → 0.8–1.1 wt% Rb_2O; <2 → 3.5–5.7 wt% F), while the contents of Al and Fe decrease in the same direction (33–35 → 24–34 wt% Al_2O_3; 2.2–3.6 → 1.4–2.2 wt% FeO). The contents of trace elements show a wide dispersion. Anyway, the medians of Sn, Nb, and Ta increase from cores to rims (200 → 260 ppm Sn, 145 → 165 ppm Nb, 12 → 37 ppm Ta), and the median of W decreases from 17 to 11 ppm. Crystal overgrowths are formed by hundreds of small grains growing mostly perpendicular to the core–rim surface, and are poor in Sn, W and Nb, but relatively enriched in Ta.

The behavior of mica during intensive greisenization, i.e., metasomatic processes, has been studied in detail at Cínovec (Breiter et al., 2019a): zinnwaldite in Li-rich greisen is homogeneous; it was well equilibrated during a hydrothermal event without any remnants of magmatic cores. On the other hand, late muscovitization connected with washing out of Li and an increase in Sn affected only the rims of mica flakes, while the zinnwaldite cores retained their original composition (Fig. 3d).

Greisenization at Beauvoir varies locally, resembling the late muscovitization from Cínovec: cores of some primary lepidolite grains are well-preserved while others are entirely replaced. Also here, the newly formed muscovite is distinctly Sn-enriched (Monnier et al., 2022).

9.5. *Are there any relations among mica chemistry and geochemical type of granites?*

As shown in previous chapters, the contents of trace elements in micas are highly variable. Still, based on ca. 2600 laser-ablation analyses, some general relations between trace-element spectra in micas and geochemical affiliation of parental granite can be deduced. Micas from peraluminous S-type RMGs are generally more strongly enriched in W and Cs, while micas from metaluminous–slightly peraluminous A-type granites are relatively enriched in Nb and Sc. Micas from the metaluminous–peralkaline Madeira pluton are rich in Nb and poor in Cs, Sc and W (Fig. 15). The contents of Sn and Ta do not correlate with either geochemical types of parental granites, nor the degree of their fractionation.

10. Conclusions

The variations observed in the chemical composition of micas can be explained by: (i) different geochemical affiliations of the parental rocks, (ii) the grade of mica evolution (biotite → zinnwaldite → lepidolite, or muscovite → lepidolite), and probably also (iii) regional geochemical specialization in some regions. Major results of our comprehensive review of ca. 2600 spot analyses can be formulated as follows:

- The contents of the rare alkalis Li, Rb and Cs, and the contents of Zn varied from tenths of ppm to several wt%; these elements are able to form mica “endmember” polylithionite (common), unnamed Rb and Cs endmembers, and hendricksite (rare). Maximum contents of rare metals reach hundreds to a few thousands of ppm: 1200 ppm Sn, 400 ppm W, 2300 ppm Nb and 600 ppm Ta.
- With increasing magma differentiation, the contents of Li and Rb in crystallizing mica increase, while the contents of HFSE usually decrease. Rather than the influence of the crystal structure, it is a consequence of the crystallization of Li-mica after crystallization of the HFSE accessories; the higher are the contents of Sn, Nb and Ta in the melt, the higher are the amounts of cassiterite and columbite crystallized, and the lower are the Sn and Nb contents in the later crystallized micas. No equilibrium rules between mica and melt can be used here.
- Micas from peraluminous RMGs are generally enriched in W and Cs, while micas from subaluminous A-type granites are relatively enriched in Nb and Sc. Micas from the subaluminous–peralkaline Madeira granites are rich in Nb, and poor in Cs, Sc and W.
- Zinnwaldite from Li-rich greisens is homogeneous; it was well equilibrated during the relatively high-temperature hydrothermal stage. Late (lower temperature) muscovitization connected with washing out of Li and an increase in Sn contents affected only rims of mica flakes but retained the original composition of zinnwaldite cores.
- In the succession from the early biotite to late zinnwaldite granites, the share of mica on the bulk contents of Sn, Nb and Ta decreases (50–80 → 5–10%, 10–80 → 1–10% and 100 → <5%, respectively),

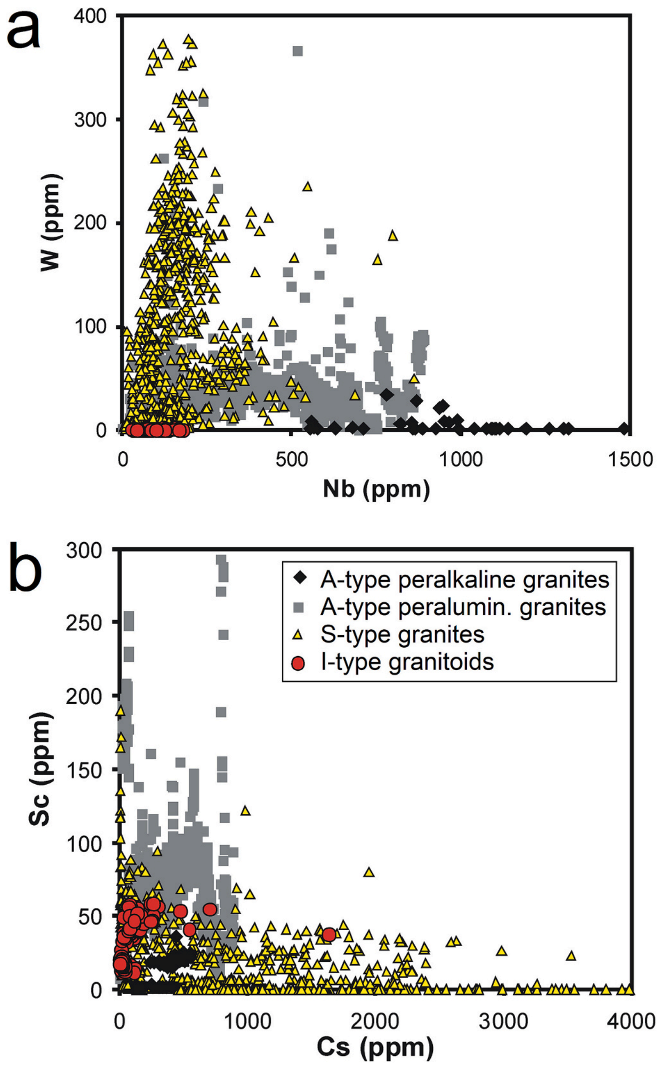

Fig. 15. Basic differences in trace-element composition of micas from RMGs of different geochemical types: a, Nb vs. W; b, Cs vs. Sc.

and rutile, cassiterite and columbite become the main hosts of rare metals.

Declaration of Competing Interest

The authors declare that they have no known competing financial interests or personal relationships that could have appeared to influence the work reported in this paper.

Acknowledgements

This study was supported by the Czech Science Foundation Project No. P210/19/05198S to Karel Breiter and Project No. EXPRO 19-29124X to Jindřich Kynický. Cooperation of Z.K. was supported by RVO 67985831 at the Institute of Geology of the Czech Academy of Sciences. Louis Raimbault and Elena Badanina are thanked for providing samples from Beauvoir and Orlovka, respectively. Inspirational reviews by two anonymous reviewers with particular remarks to the Beauvoir granite and South Bohemian batholith are acknowledged.

Appendix A. Supplementary data

Supplementary data to this article can be found online at https://doi.org/10.1016/j.lithos.2023.107135.

References

Badanina, E.V., Veksler, I.V., Thomas, R., Syritso, L.F., Trumbull, R.B., 2004. Magmatic evolution of Li-F rare-metal granites: a case study of melt inclusions in the Khangilay complex, Eastern Transbaikalia (Russia). Chem. Geol. 210, 113–133.

Bailey, S.W., 1984. Micas. Rev. Mineral. 13, 1–584.

Bastos Neto, A.C., Pereira, V.P., Ronchi, L.H., Lima, E.F., Frantz, J.C., 2009. The world-class Sn, Nb, Ta, F (Y, REE, Li) deposit and the massive cryolite associated with the albite-enriched facies of the Madeira A-type granite, Pitinga mining district, Amazonas State, Brazil. Can. Mineral. 47, 1329–1357.

Bea, F., Pereira, M.D., Stroh, A., 1994. Mineral/leucosome partitioning in a peraluminous migmatite (a laser ablation–ICP–MS study). Chem. Geol. 117, 291–312.

Bonin, B., 2007. A-type granites and related rocks: evolution of a concept, problems and prospects. Lithos 97, 1–29.

Borges, R.M.K., Villas, R.N.N., Fuzikawa, K., Dall'Agnol, R., Pimenta, M.A., 2009. Phase separation, fluid mixing, and origin of the greisens and potassic episyenite associated with the Água Boa pluton, Pitinga tin province, Amazonian Craton, Brazil. J. S. Am. Earth Sci. 27, 161–183.

Breiter, K., 2012. Nearly contemporaneous evolution of the A- and S-type fractionated granites in the Krušné hory/Erzgebirge Mts., Central Europe. Lithos 151, 105–121.

Breiter, K., Koller, F., 1999. Two-mica granites in the central part of the South Bohemian Pluton. Abh. Geol. Bundesanst. 56, 201–212.

Breiter, K., Koller, F., 2009. Mafic K- and Mg-rich magmatic rocks from Western Mühlviertel (Austria) area and the adjacent part of the Šumava Mountains (Czech Republic). Jahrb. Geol. Bundesanst. 149, 477–485.

Breiter, K., Förster, H.-J., Seltmann, R., 1999. Variscan silicic magmatism and related tin-tungsten mineralization in the Erzgebirge-Slavkovský les metallogenic province. Mineral. Deposita 34, 505–521.

Breiter, K., Müller, A., Leichmann, J., Gabašová, A., 2005. Textural and chemical evolution of a fractionated granitic sytem: the Podlesí stock, Czech Republic. Lithos 80, 323–345.

Breiter, K., Koller, F., Scharbert, S., Siebel, W., Škoda, R., Frank, W., 2007. Two-mica granites of the Plechý (Plockenstein) pluton in the Triple-point area of Austria, the Czech Republic and Germany. Jahrb. Geol. Bundesanst. 147, 527–544.

Breiter, K., Vaňková, M., Vašinová Galiová, M., Korbelová, Z., Kanický, V., 2017a. Lithium and trace element concentrations in trioctahedral micas from granites of different geochemical types meassured via laser ablation ICP-MS. Mineral. Mag. 81, 15–33.

Breiter, K., Ďurišová, J., Hrstka, T., Korbelová, Z., Hložková Vaňková, M., Vašinová Galiová, M., Kanický, V., Rambousek, P., Knésl, I., Dobeš, P., Dosbaba, M., 2017b. Assessment of magmatic vs. metasomatic processes in rare-metal granites: a case study of the Cínovec-Zinnwald Sn–W–Li deposit, Central Europe. Lithos 292, 198–217.

Breiter, K., Hložková, M., Korbelová, Z., Vašinová Galiová, M., 2019a. Diversity of lithium mica compositions in mineralized granite–greisen system: Cínovec Li-Sn-W deposit, Erzgebirge. Ore Geol. Rev. 106, 12–27.

Breiter, K., Badanina, E., Ďurišová, J., Dosbaba, M., Syritso, L., 2019b. Chemistry of quartz: A new insight into the origin of the Orlovka Ta-Li deposit, Eastern Transbaikalia, Russia. Lithos 348–349, 105206.

Breiter, K., Ďurišová, J., Korbelová, Z., Lima, A., Vašinová Galiová, M., Hložková, M., Dosbaba, M., 2022. Rock textures and mineral zoning – A clue to understanding rare-metal granite evolution: Argemela stock, Central-Eastern Portugal. Lithos 410–411, 106562.

Breiter, K., Ďurišová, J., Korbelová, Z., Vašinová Galiová, M., Hložková, M., 2023. Granite pluton at the Panasqueira tungsten deposit, Portugal: genetic implications as revealed from new geochemical data. Minerals 13, 163.

Černý, P., Burt, D., 1984. Paragenesis, crystallochemical characteristics, and geochemical evolution of micas in granite pegmatites. Rev. Mineral. 13, 257–297.

Černý, P., Meintzer, R.E., Anderson, A.J., 1985. Extreme fractionation in rare-element granitic pegmatites: selected examples of data and mechanisms. Can. Mineral. 23, 381–421.

Černý, P., Chapman, R., Teerstra, D.K., Novák, M., 2003. Rubidium- and cesium-dominant micas in granitic pegmatites. Am. Mineral. 8, 1832–1835.

Chappell, B.W., White, A.J.R., 1974. Two contrasting granite types. Pac. Geol. 8, 173–174.

Charoy, B., Noronha, F., 1996. Multistage growth of a rare-element, volatile-rich microgranite at Argemela (Portugal). J. Petrol. 37, 73–94.

Christiansen, E.H., Haapala, I., Hart, G.L., 2007. Are Cenozoic topaz rhyolites the erupted equivalents of Proterozoic rapakivi granites? Examples from the western United States and Finland. Lithos 97, 219–246.

Costi, H.T., Dall'Agnol, R., Moura, C.A.V., 2000. Geology and Pb-Pb geochronology of Paleoproterozoic volcanic and granitic rocks of Pitinga province, Amazonian craton, northern Brazil. Int. Geol. Rev. 42, 832–849.

Costi, H.T., Dall'Agnol, R., Pichavant, M., Rämö, O.T., 2009. The peralkaline tin-mineralized Madeira cryolite albite-rich granite of Pitinga, Amazonian craton, Brazil: petrography, mineralogy and crystallization processes. Can. Mineral. 47, 1301–1327.

Cuney, M., Marignac, C., Weisbrod, A., 1992. The Beauvoir topaz-lepidolite albite granite (Massif Central, France): the disseminated magmatic Sn-Li-Ta-Nb-be mineralization. Econ. Geol. 87, 1766–1794.

Dall'Agnol, R., Frost, C.D., Ramo, T., 2012. IGCP Project 510 "A-type Granites and Related Rocks through Time": Project vita, results, and contribution to granite research. Lithos 151, 1–16.

Eby, G.N., 1992. Chemical subdivision of A-type granitoids: petrogenetic and tectonic implications. Geology 20, 641–644.

Finger, F., Clemens, J.D., 2002. Cadomian lower-crustal contribution to Variscan petrogenesis (South Bohemian Batholith, Austria): a comment. J. Petrol. 43, 1779–1781.

Foster, M.D., 1960. Interpretation of the composition of Li-micas. U.S. Geol. Surv. Prof. Pap. 354E, 113–147.

Frondel, C., Baum, J.L., 1974. Structure and mineralogy of the Franklin zinc-iron–manganese deposit, New Jersey. Econ. Geol. 69, 157–180.

Frost, C.D., Ramo, T., Dall'Agnol, R., 2007. IGCP project 510 – A-type granites and related rocks through time. Lithos 97 vii–xiii.

Gerdes, A., Friedl, G., Parrish, R.R., Finger, F., 2003. High-resolution geochronology of Variscan granite emplacement – the South Bohemian Batholith. J. Czech Geol. Soc. 48, 53–54.

Goldschmidt, V.M., 1937. The principles of distribution of chemical elements in minerals and rocks. J. Chem. Soc. 1937, 655–673.

Goodenough, K.M., Upton, B.G.J., Ellam, R.M., 2000. Geochemical evolution of the Ivgtut granite, South Greenland: a fluorine-rich "A-type" intrusion. Lithos 51, 205–221.

Haapala, I., 1995. Metallogeny of the rapakivi granites. Mineral. Petrol. 54, 149–160.

Haapala, I., Frindt, S., Kandara, J., 2007. Cretaceous Gross Spitzkoppe and Klein Spitzkoppe stocks in Namibia: Topaz-bearing A-type granites related to continental rifting and mantle plume. Lithos 97, 174–192.

Holub, F.V., 1997. Ultrapotasic plutonic rocks of the durbachite series in the Bohemian Massif: petrology, geochemistry and petrogenetic interpretation. J. Geol. Sciences. Econ. Geol. Mineral. 31, 5–26.

Holub, F.V., Machart, J., Manová, M., 1997. The Central Bohemian plutonic complex. J. Geol. Sciences. Econ. Geol. Mineral. 31, 27–49.

Hrstka, T., Gottlieb, P., Skála, R., Breiter, K., Motl, D., 2018. Automated mineralogy and petrology – applications of TESCAN Integrated Mineral Analyzer (TIMA). J. Geosci. 63, 47–63.

Icenhower, J., London, P., 1995. An experimental study of element partitioning among biotite, muscovite, and coexisting peraluminous silicic melt at 200 MPa (H_2O). Am. Mineral. 80, 1229–1251.

Icenhower, J., London, D., 1996. Experimental partitioning of Rb, Cs, Sr, and Ba between alkali feldspars and peraluminous melt. Am. Mineral. 81, 719–734.

Johan, Z., Strnad, L., Johan, V., 2012. Evolution of the Cínovec (Zinnwald) granite cupola, Czech Republic: composition of feldspars and micas, a clue to the origin of W, Sn mineralization. Can. Mineral. 50, 1131–1148.

Koller, F., Breiter, K., 2003. Variations of Li-, Be-, Rb-, and Sn-contents in micas from Variscan granites of the South Bohemian Pluton. LERM 2003. In: International Symposium on Light Elements in Rock-forming Minerals. Nové Město na Moravě. Book of Abstracts, pp. 40–41.

Launay, G., Sizaret, S., Lach, P., Melleton, J., Gloaguen, E., Poujol, M., 2021. Genetic relationship between greisenization and Sn-W mineralizations in vein and greisen deposits: Insights from the Panasqueira deposit (Portugal). BSGF—Earth. Sci. Bull. 192, 2.

Legros, H., Marignac, C., Tabary, T., Mercadier, J., Richard, A., Cuney, M., Wang, R.C., Charles, N., Lespinasse, M.Y., 2018. The ore-forming magmatic-hydrothermal system of the Piaontang W-Sn deposit (Jiangxi, China) as seen from Li-mica geochemistry. Am. Mineral. 103, 39–54.

Li, J., Huang, X.L., He, P.-L., Li, W.X., Chen, L., 2015. In situ analyses of micas in the Yashan granite, South China: constraints on magmatic and hydrothermal evolutions of W and Ta-Nb bearing granites. Ore Geol. Rev. 65, 793–810.

Loiselle, M.C., Wones, D., 1979. Characteristics and origin of anorogenic granites. Geol. Soc. Am. Abstr. Programs 11, 468.

Lukkari, S., Thomas, R., Haapala, I., 2009. Crystallization of the Kymi topaz granite stock within the Wiborg rapakivi batholith, Finland: evidence from melt inclusions. Can. Mineral. 47, 1359–1374.

Marignac, C., Cuney, M., Cathelineau, M., Lecomte, A., Carocci, E., Pinto, F., 2020. The Panasqueira rare metal granite suites and their involvement in the genesis of the world-class Panasqueira W-Sn-Cu deposit: a petrographic, mineralogical, and geochemical study. Minerals 10, 562.

Martin, R.F., 2006. A-type granites of crustal origin ultimately result from open-system fenitization-type reactions in an extensional environment. Lithos 91, 125–136.

McDonough, W.F., Sun, S., 1995. The composition of the Earth. Chem. Geol. 120, 223–253.

Merlet, C., 1994. An accurate computer correction program for quantitative electron probe microanalysis. Microchim. Acta 114 (115), 363–376.

Michaud, J.A.S., Pichavant, M., 2020. Magmatic fractionation and the magmatic-hydrothermal transition in rare metal granites: evidence from Argemela (Central Portugal). Geochim. Cosmochim. Acta 289, 130–157.

Monier, G., Robert, J.-L., 1986. Evolution of the miscibility gap between muscovite and biotite solid solutions with increasing lithium content: an experimental study in the system K_2O–Li_2O–MgO–FeO–Al_2O_3–SiO_2–H_2O–HF– at 600 °C, 2 kbar P_{H2O}: comparison with natural lithium micas. Mineral. Mag. 50, 641–651.

Monier, G., Charoy, B., Cuney, M., Ohnenstetter, D., Robert, J.L., 1987. Évolution spatiale et temporelle de la composition des micas du granite albitigue a topaze-lépidolite de Beauvoir. Geol. Fr. 2–3, 179–188.

Monnier, L., Salvi, S., Melleton, J., Lach, P., Pochon, A., Baily, L., Béziat, D., De Parseval, P., 2022. Mica trace-element signatures: highlighting superimposed W-Sn mineralizations and fluid sources. Chem. Geol. 600, 120866.

Mottana, A., Sassi, F.P., Thompson Jr., J.B., Guggenheim, S. (Eds.), 2002. Micas: crystal chemistry & metamorphic petrology. Rev. Mineral. Geochem. 46, 1–499.

Paludo, C.M., Bastos Neto, A.C., Pereira, V.P., Botelho, N.F., 2018. Mineralogia e geoquímica de pegmatitos ricos em ETR, F e metais alcalinos associados à facies albita granito no depósito de Sn-Nb-Ta- (F, ETR, U, Th) Madeira (mina Pitinga, AM, Brasil). Pesquisas em Geociências 45, e0747.

Pearce, J.A., Harris, N.B.W., Tindle, A.G., 1984. Trace element discrimination diagrams for the tectonic interpretation of granitic rocks. J. Petrol. 25, 956–983.

Raimbault, L., Cuney, M., Azencott, C., Duthou, J.L., Joron, J.L., 1995. Geochemical evidence for a multistage magmatic genesis of Ta–Sn–Li mineralization in the granite at Beauvoir, French Massif Central. Econ. Geol. 90, 548–596.

Rieder, M., 2001. Mineral nomenclature in the mica group: the promise and the reality. Eur. J. Mineral. 13, 1009–1012.

Roda-Robles, E., Pesquera, A., Gil-Crespo, P., Torres-Ruiz, J., 2012. From granite to highly evolved pegmatite: a case study of the Pinilla de Fermoselle granite-pegmatite system (Zamora, Spain). Lithos 153, 192–207.

Seltmann, R., Schilka, W., 1991. Metallogenetic aspects of breccia-related tin granites in the Eastern Erzgebirge. Z. Geol. Wiss. 19, 485–490.

Shand, S.J., 1943. Eruptive Rocks. Their Genesis Composition Classification, and their Relation to Ore-Deposits. John Wiley & Sons, New York.

Siebel, W., Shang, C.K., Reitter, E., Rohrmüller, J.K., Breiter, K., 2008. Two distinctive granite suites in the south-western Bohemian Massif and their record of emplacement: constraints from zircon $^{207}Pb/^{206}Pb$ chronology and geochemistry. J. Petrol. 49, 1853–1872.

Štemprok, M., 1987. Greisenization (a review). Geol. Rundsch. 76, 169–175.

Stepanov, A.S., Hermann, J., 2013. Fractionation of Nb and Ta by biotite and phengite: implications for the missing Nb paradox. Geology 41, 303–306.

Taylor, R.P., Fallick, A.E., 1997. The evolution of fluorine-rich felsic magmas: source dichotomy, magmatic convergence and the origins of topaz granite. Terra Nova 9, 105–108.

Tichomirowa, M., Leonhardt, D., 2010. New age determinations (Pb/Pb zircon evaporation, Rb/Sr) on the granites from Aue-Schwarzenberg and Eibenstock, Western Erzgebirge, Germany. Z. Geol. Wiss. 38, 99–123.

Tichomirowa, M., Käßner, A., Repstock, A., Weber, S., Gerdes, A., Whitehouse, M., 2022. New CA-ID-TIMS U–Pb zircon ages for the Altenberg–Teplice Volcanic Complex (ATVC) document discrete and coeval pulses of Variscan magmatic activity in the Eastern Erzgebirge (Eastern Variscan Belt). Int. J. Earth Sci. 111, 1885–1908.

Tindle, A.G., Webb, P.C., 1990. Estimation of lithium contents in trioctahedral micas using microprobe data: application to micas from granitic rocks. Eur. J. Mineral. 2, 595–610.

Tischendorf, G., Förster, H.-J., Gottesmann, B., 2001. Minor and trace-element composition of trioctahedral micas: a review. Mineral. Mag. 65, 249–276.

Van Lichtervelde, M., Grégoire, M., Linnen, R.L., Béziat, D., Salvi, S., 2008. Trace element geochemistry by laser ablation ICP-MS of micas associated with Ta mineralization in the Tanco pegmatite, Manitoba, Canada. Contrib. Mineral. Petrol. 155, 791–806.

Wang, R.C., Hu, H., Zhang, A.C., 2004. Pollucite and the cesium-dominant analoque of polylithionite as expressions of extreme Cs enrichment in the Yichun topaz-lepidolite granite, Southern China. Can. Mineral. 42, 883–896.

Warr, L.N., 2021. IMA–CNMMC approved mineral symbols. Mineral. Mag. 85, 291–320.

Whalen, J.B., Currie, K.L., Chappell, B.W., 1987. A-type granites: geochemical characteristics, discrimination and petrogenesis. Contrib. Mineral. Petrol. 95, 407–419.

Xie, L., Wang, R.C., Groat, L.A., Zhu, J.C., Huang, F.F., Cempírek, J., 2015. A combined EMPA and LA-ICP-MS study of Li-bearing mica and Sn–Ti oxide minerals from the Qiguling topaz rhyolite (Qitianling district, China): the role of fluorine in origin of tin mineralization. Ore Geol. Rev. 65, 779–792.

Zhu, Z., Wang, R., Marignac, C., Cuney, M., Mercadier, J., Che, X., Lespinasse, M.Y., 2018. A new type of rare metal granite with Nb-rich mica: the early cretaceous Huangshan rare-metal granite suite, Northeast Jiangxi Province, China. Am. Mineral. 103, 1530–1544.